INTERNATIONAL YEAR OF LIGHT 2015

4th Intl Conference on Photonics, Optics and Laser Technology (PHOTOPTICS 2016)

Keynote Lecture

Light-matter interactions in whispering-gallery-mode microresonators

Giancarlo C. Righini

Enrico Fermi Centre, Rome
Nello Carrara Institute of Applied Physics, Florence
Italy

CENTRO FERMI
Museo Storico della Fisica e Centro Studi e Ricerche Enrico Fermi

IFAC

Motivation

"... *si vede, nel diminuire i corpi non si diminuir con la medesima proporzione le forze, anzi ne i minimi crescer la gagliardìa con proporzion maggiore ...*

"... one can note that smaller bodies in nature are not just scaled replicas of similar bigger objects but, on the contrary, they have enhanced properties ..."

Galileo, "Discorsi e Dimostrazioni Matematiche intorno a due Nuove Scienze"

"Dialogue Concerning Two New Sciences" (1638)

- Resonant cavities are structures of outmost importance in optics. Just to make an example, laser would not exist without an optical cavity.
- The interaction of matter and light can be dramatically increased by the presence of a microcavity.
- A kind of optical cavity which has attracted an increasing interest in the last two decades, even if the principle is known since more than a century, is the one which is based on WGMs (Whispering Gallery Modes).

Outline

Light-matter interactions in whispering-gallery-mode microresonators

- Basics of Whispering Gallery Mode Resonators (WGMR)
- Microspherical (Bulk and Hollow) Resonators (ms-WGMR)
- Lasing in ms-WGMRs
- Nonlinear Optics in ms-WGMRs
- Biosensing by ms-WGMRs
- Outlook

Whispering Gallery Modes (WGM)

The Whispering Gallery phenomenon was first described in 1910 by Lord Rayleigh, based on observations in St. Paul's Cathedral in London.

A person just whispering close to the wall can be heard all the way along the gallery, more than 40 m to the other side, due to the sound reflections along the circular wall.

Lord Rayleigh
(1842 – 1919)

L. Rayleigh, "The Problem of the Whispering Gallery", Philosophical Magazine 20, 1001–1004 (1910).

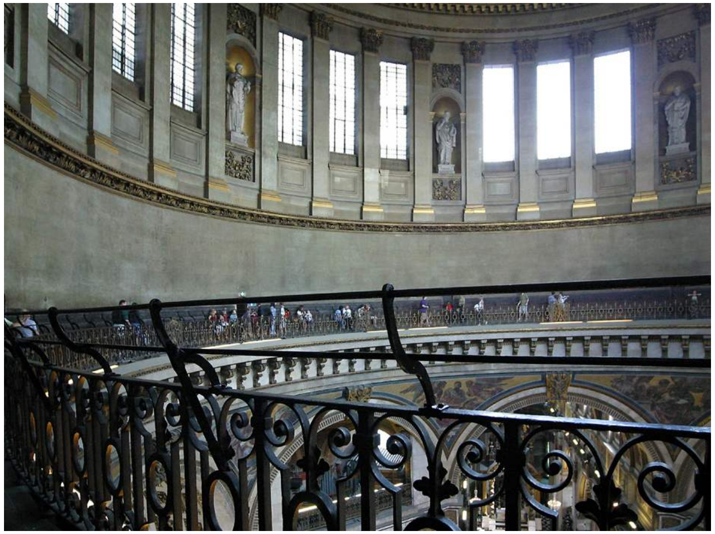

Whispering Gallery under the cupola of the St. Paul's Cathedral in London

Whispering Gallery

Optical: total internal reflection

TIR $\Rightarrow$ $i > i_c = \arcsin(1/N)$

+ phase matching after a round-trip

Resonance Condition: $2 \pi R N = l \lambda$

Acoustic:
reflection
from surface

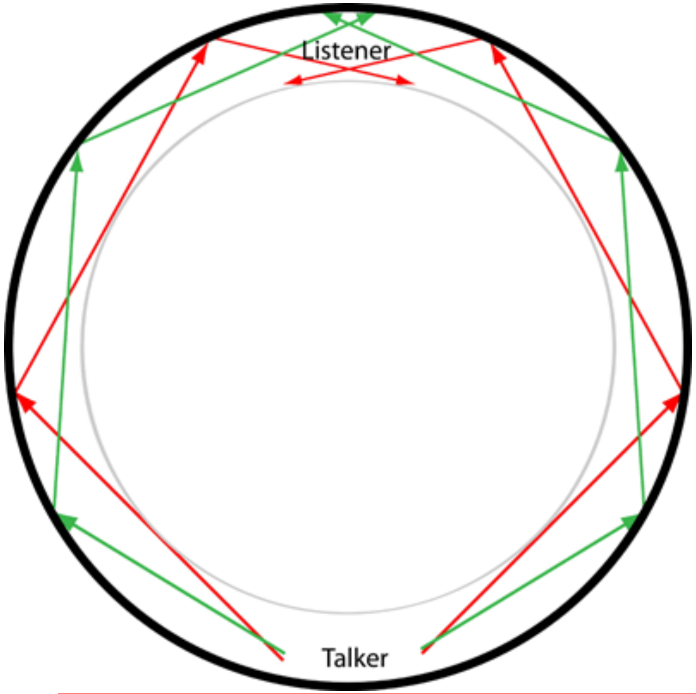

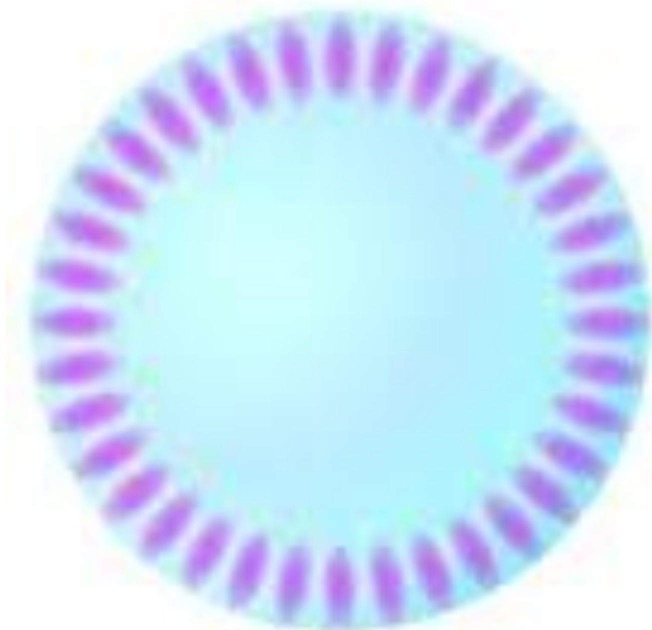

Image credit: Ivan Grudinin

Whispering Gallery Modes

Wave Approach

WGM = defined by *n, l, m* and polarization (TE,TM)

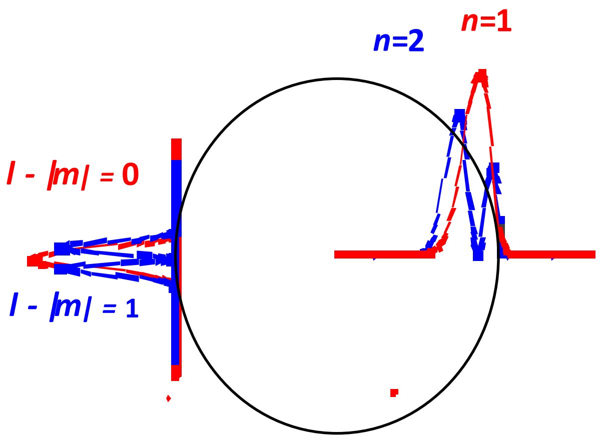

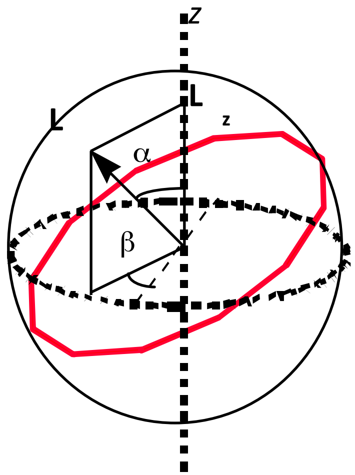

- ***n*** *radial mode number* corresponds to the number of maxima along the radial direction
- ***l*** *angular mode number* depends on the equatorial length, expressed in number of wavelengths
- ***m*** *azimuthal mode number* **$-l < m < l$**
- **$l-|m|+1$** gives the number of maxima along the polar direction.

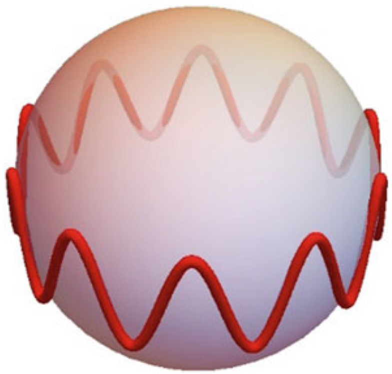

WGMs can be solved numerically

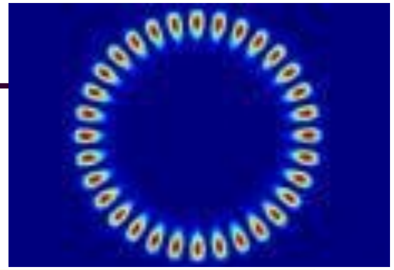

E_{lmq} = Numerical solutions (FEM, FDTD)

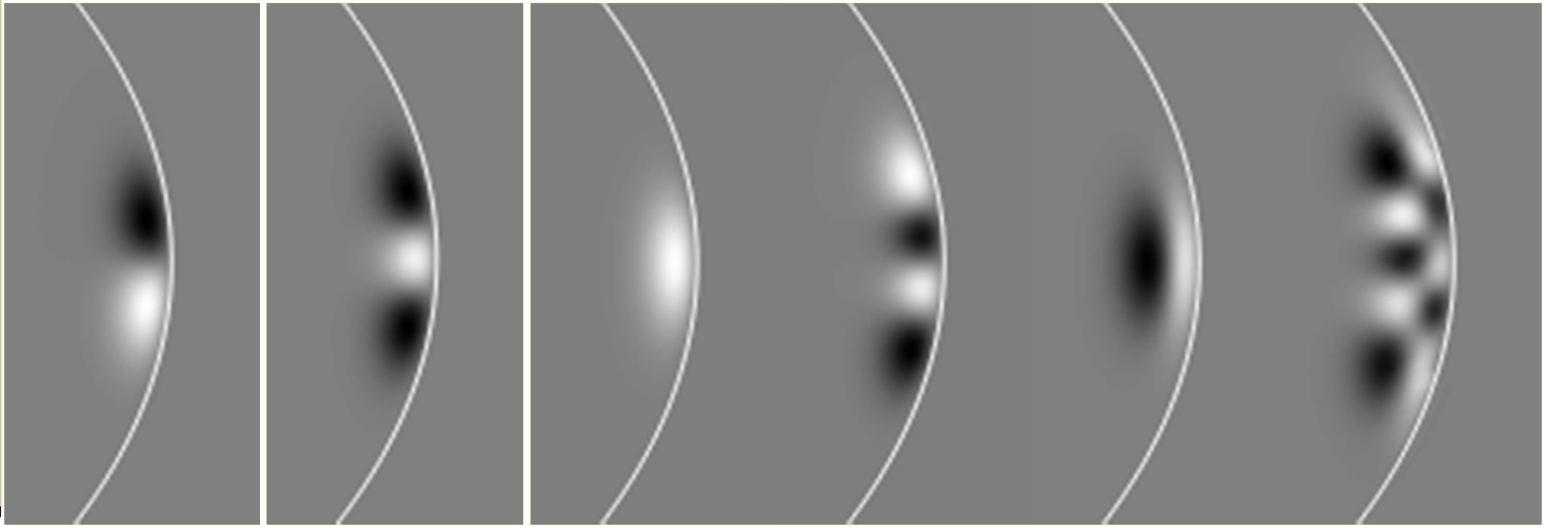

l-m=1,q=1 l-m=2,q=1 l=m, q=1 l-m=3,q=1 l-m=1,q=2 l-m=4,q=2

E_{lmq}, color ~ radial component of electric field

50x100 μm window, TM modes

Image credit: Ivan Grudinin

Modes in a spherical geometry

n = 1, 2, 3

l–m+1 = 1, 5, 9

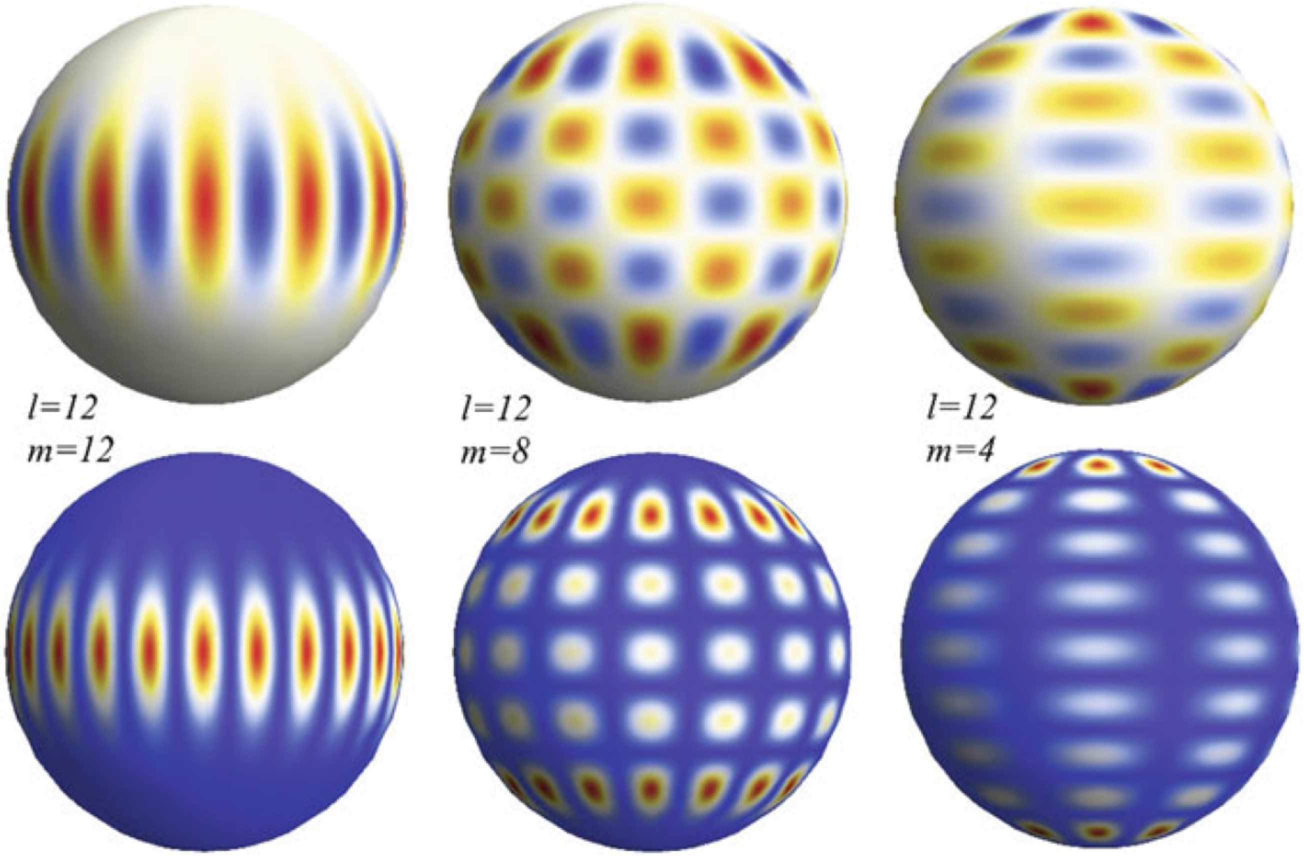

Electric field amplitudes (top row) and intensities (bottom row) for the 3 first-order radial modes with the same *l* but different *m*.

*Adapted from A. Francois et al., Chapt. 9, in "*Photonic Materials for Sensing, Biosensing and Display Devices" (springer, 2015)

WGMR parameters

$$Q = \frac{\omega_0}{\delta\omega}$$

Free spectral range (Δf_{fsr}): The difference in frequency between adjacent modes.

$$\Delta f_{fsr} \approx \frac{c}{2\pi Na}\frac{\tan^{-1}\left(\sqrt{N_{eff}^2 - 1}\right)}{\sqrt{N_{eff}^2 - 1}}$$

Finesse ($\mathcal{F}$): The finesse is the ratio of the free spectral range to the resonance peak width.

$$F = \frac{\Delta f_{fsr}}{\Delta f} = Q\frac{\Delta f_{fsr}}{f_0} = Q\frac{\Delta\lambda_{fsr}}{\lambda_0}.$$

Mode volume (V_m): The mode volume represents the volume occupied by the resonant mode field.

$$V_m \approx 3.4\pi^{3/2}\left(\frac{\lambda_0}{2\pi N}\right)^3 l^{11/6}\sqrt{l - m + 1}$$

WGM Devices

7 February 2002
International weekly journal of science
nature
www.nature.com
A compact silica laser
Marine bacteria
Mystery microbes prove versatile
Ocean circulation
A 30-year Pacific slowdown
Genome shuffling
Improving the breed
Malaria
Nature Insight
naturejobs

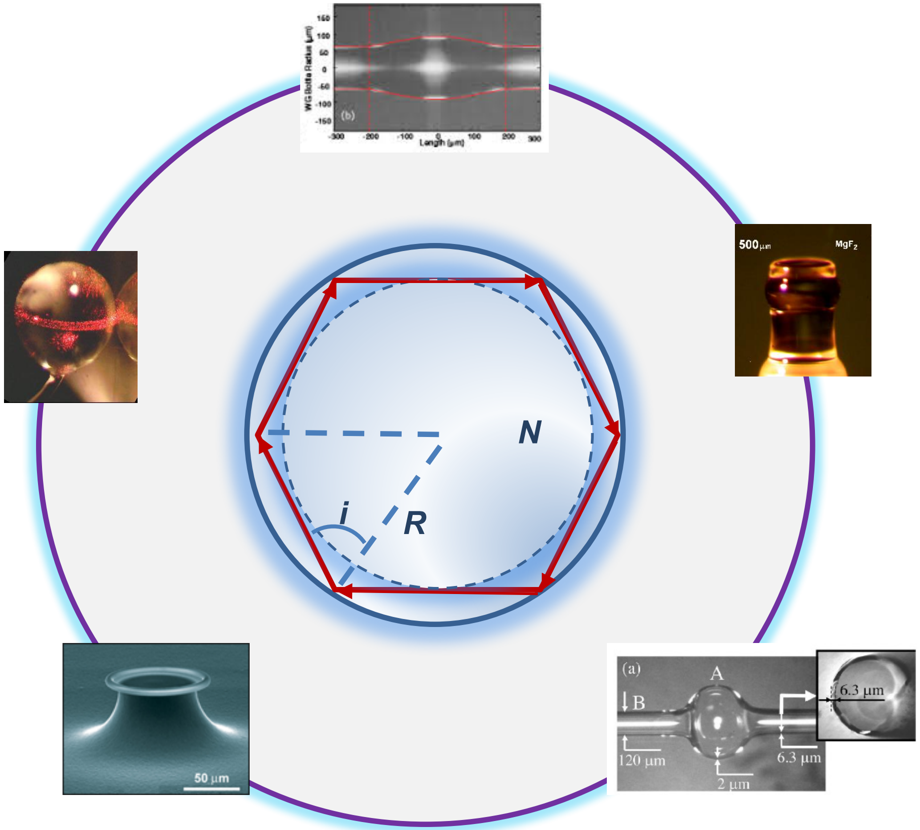

150
100
50
0
-50
-100
-150
(b)
-300
-200
-100
0
100
200
300
Length (μm)
500 μm
MgF_2
N
i
R
50 μm
(a)
A
B
6.3 μm
120 μm
6.3 μm
2 μm

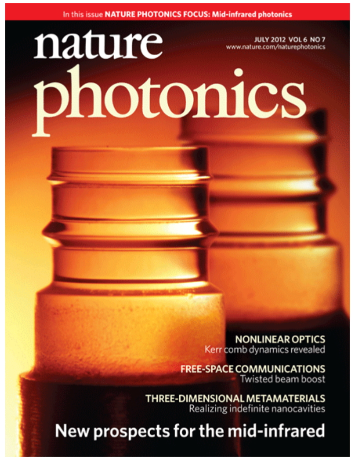

In this issue NATURE PHOTONICS FOCUS: Mid-infrared photonics
nature photonics
JULY 2012 VOL 6 NO 7
NONLINEAR OPTICS
Kerr comb dynamics revealed
FREE-SPACE COMMUNICATIONS
Twisted beam boost
THREE-DIMENSIONAL METAMATERIALS
Realizing indefinite nanocavities
New prospects for the mid-infrared

27 February 2003
International weekly journal of science
nature
www.nature.com/nature
Disk world
Resonators on a chip bring microphotonics closer
Tumour suppressors
Unexpected role for retinoblastoma gene
Circadian clocks
Time for antisense RNA
String theory
Hidden dimensions still in hiding
naturejobs physics meets biology

nature methods
Techniques for life scientists and chemists

WGMR Geometries

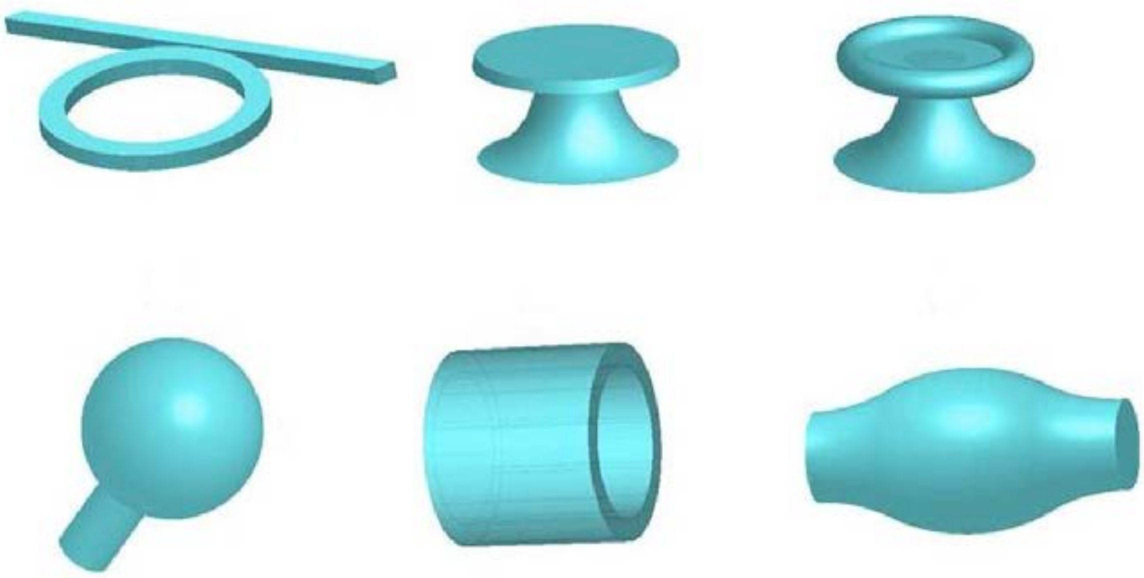

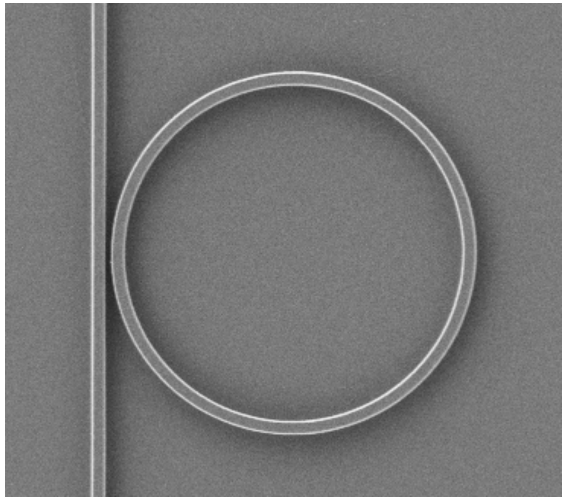

K. Preston *et al.*, *Opt. Exp.* 2007

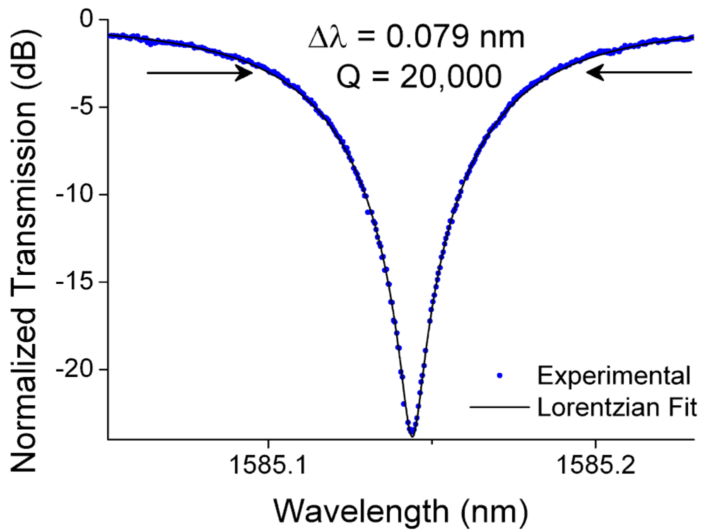

For all WGM resonators a key parameter is the quality factor:

$$Q = \nu / d\nu = 2\pi N_{eff} / \alpha\lambda$$

$$(10^4 - 10^9)$$

WGMR Best Values

*$\mathcal{F}$ and **Q** are typically equally important in most applications. In some cases, however, finesse is technically more valuable than the quality factor.*

Theory predicts for crystalline WGMRs the possibility of achieving ***Q*** close to 10^{14} and corresponding $\mathcal{F}$ higher than 10^{9}. Measured values are smaller, but a CaF_2 WGMR with ***Q*** > 10^{11} and $\mathcal{F}$ > 10^{7} was demonstrated at 1.55 μm wavelength.[1]

For spherical WGMRs in silica, top values of ***Q*** 10^{10} and $\mathcal{F}$ > 10^{6} at 0.85 μm wavelength were also measured. [2]
Values of ***Q*** > 10^{8} are routinely achieved. [3]

[1] A. A. Savchenkov *et al.,* Opt. Express 15, 6768 (2007)
[2] D. W. Vernooy *et al.*, Physi. Review A, 57, R2293 (1998)
[3] A. Chiasera *et al.,* Laser & Photonics Rev. 4, 457 (2010)

Spherical microresonators

Among the various types of 3D WGM microresonators (WGMR), the **spherical** one is the simplest to fabricate and the one with higher Q (> 10^8).

Its very high Q and the critical morphology dependence makes this WGMR particularly suitable to both **nonlinear optics** experiments and implementation of **sensors** with very high accuracy.

Figure 4 (online color at: www.lpr-journal.org) Upconversion green image mapping the optical pump WGMs in an erbium-doped phosphate microsphere with a diameter of approximately 150 micrometers.

A. Chiasera, Y. Dumeige, P. Féron, M. Ferrari, Y. Jestin, G. Nunzi Conti, S. Pelli, S. Soria, and G.C. Righini."Spherical whispering-gallery-mode microresonators", Laser & Photonics Reviews 4 (2010) pp. 457-482

G.C. Righini, Y. Dumeige, P. Féron, M. Ferrari, G. Nunzi Conti, D. Ristic, S. Soria., "Whispering gallery mode microresonators: fundamentals and applications", Rivista del Nuovo Cimento 34 (2011) pp. 435-488.

Fabrication of a microsphere

A simple and effective method is based on the melting (usually by a fiber fusion splicer or by a CO_2 laser) of the end of a standard telecom fiber.

In our lab the end of an SMF-28 optical fiber is partially fused by the arc discharge generated between the two metal electrodes. Due to the surface tension, the optical microsphere is formed.

150 – 250 μm silica optical microspheres **Q ~ 10^8**

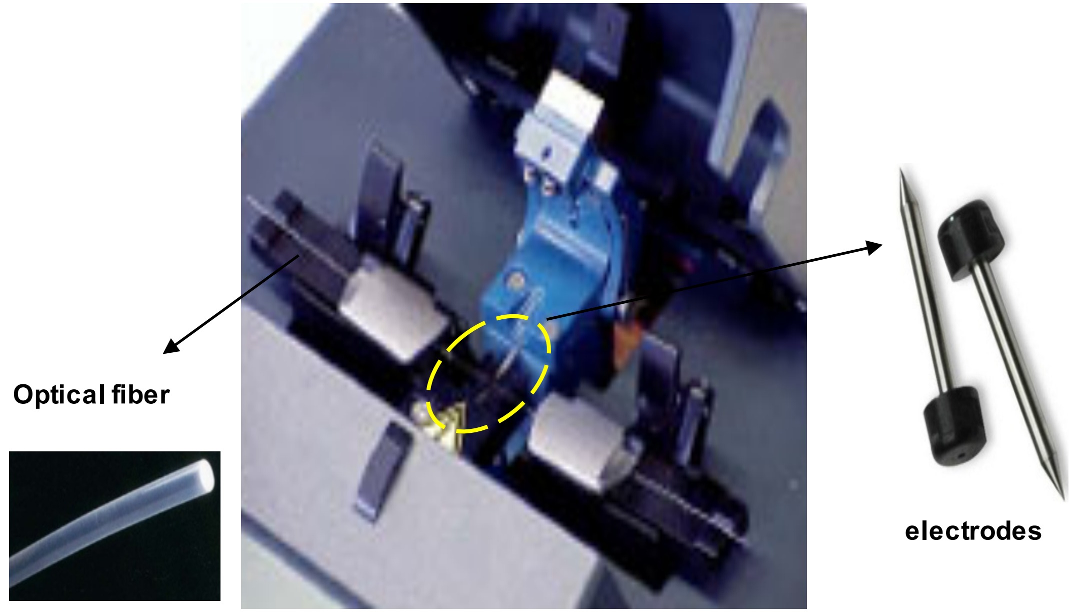

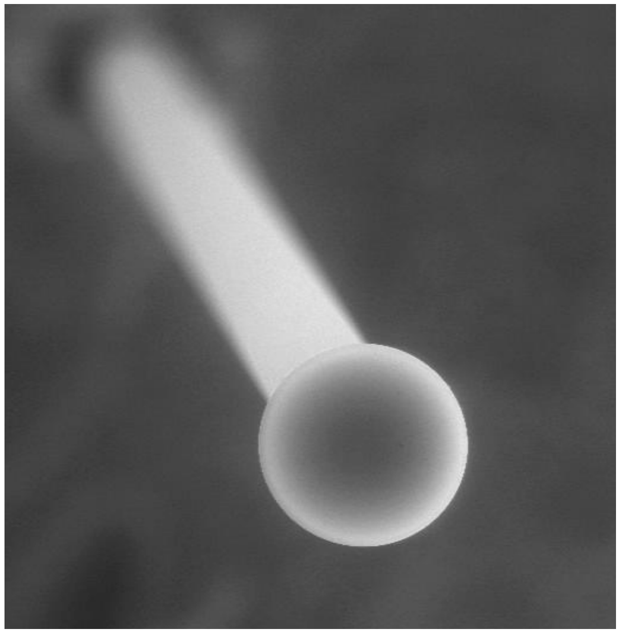

Fabrication from composite glasses

BUT …non-silica microspheres have to be fabricated by other methods !!

e.g.:

1) **Glass grinding**

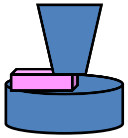

2) **Melting by a plasma torch**

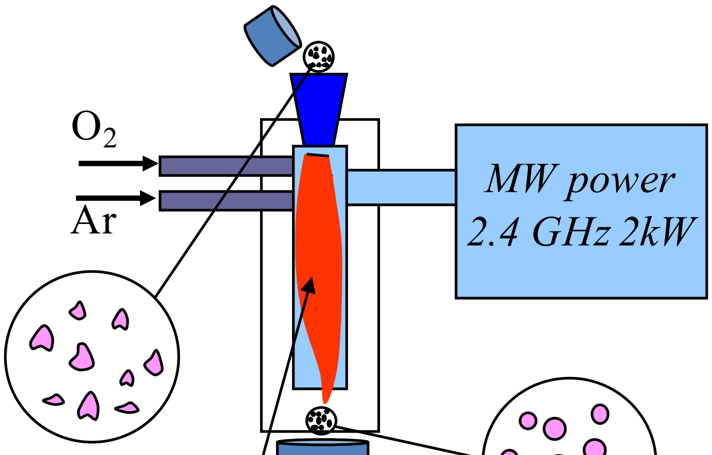

Selecting and handling

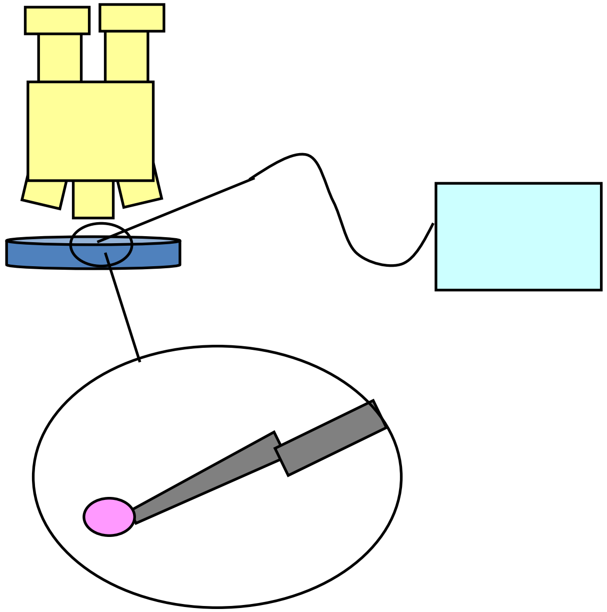

Each sphere is measured by using a microscope and glued to the end of an optical fiber.

All types of glasses can be chosen

microwave plasma torch

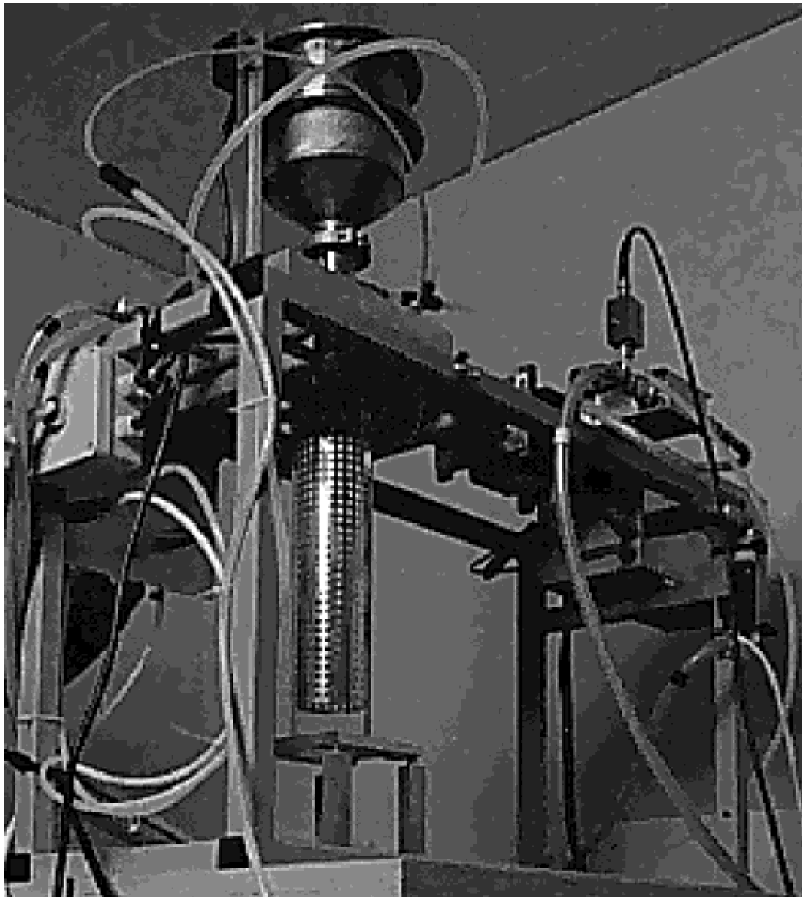

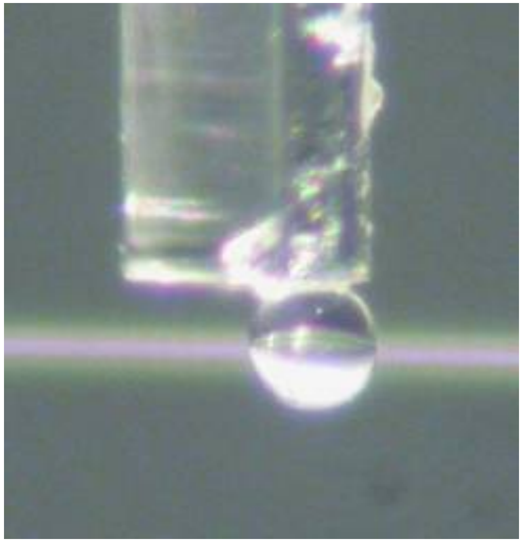

G. Nunzi Conti, A. Chiasera, L. Ghisa, S. Berneschi, M. Brenci, Y. Dumeige, S. Pelli, S. Sebastiani, P. Féron, M. Ferrari, and G. C. Righini
J. Non-Cryst. Solids 322, 2360 (2006).

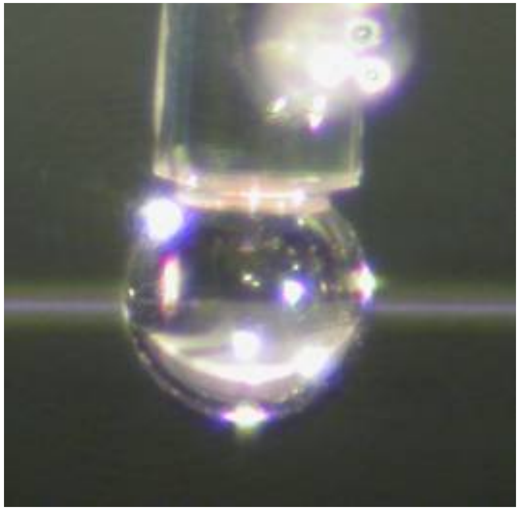

Bulk Glasses → Powders → Spheres (10 – 200 μm)

Light coupling to WGMR

Coupling occurs via evanescent wave

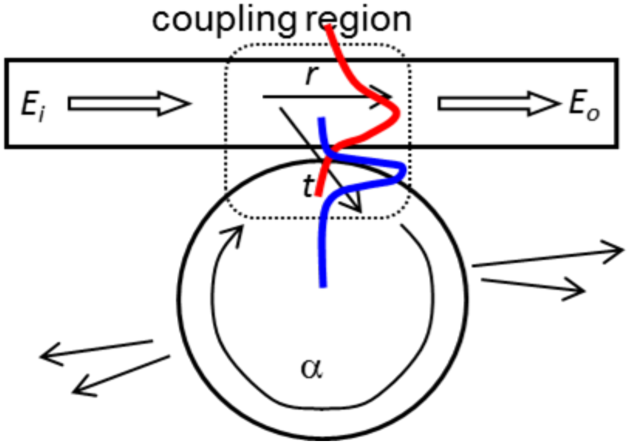

Phase Matching : $\beta_{fiber} = \beta_{sphere}$

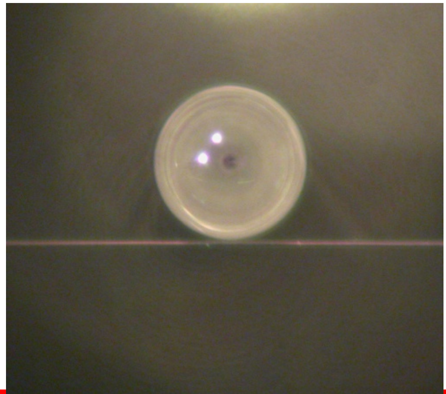

Coupling options

All methods exploit evanescent wave coupling

Tapered fiber [2]

- ☺ Efficient
- ☺ Flexible ⇒ fine tuning of coupling
- ☹ Fragile

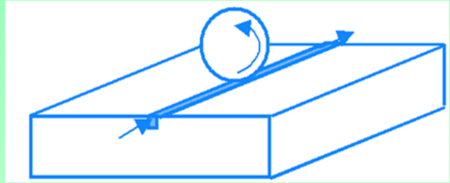

Channel waveguide [3]

- ☺ Robust
- ☺ Compact
- ☹ Efficient coupling more critical

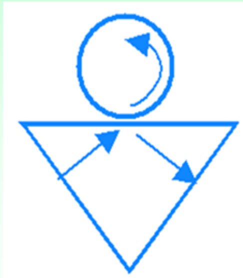

Prism

- ☺ Robust
- ☹ Alignment very critical

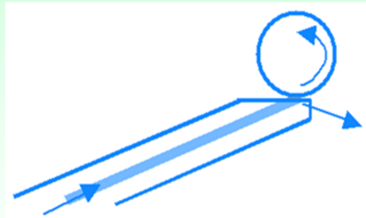

Angle-polished fiber

- ☺ Robust
- ☺ Compact
- ☺ Easy alignment
- ☹ Limited by refractive index of fibres

Tapered fiber coupling

D. Ristić, A. Rasoloniaina, A, Chiappini, P. Féron, S. Pelli, G. Nunzi Conti, M. Ivanda, G.C. Righini, G. Cibiel, and M. Ferrari *"About the role of phase matching between a coated micro-sphere and a tapered fiber: experimental study"* Optics Express, 21 (2013), 20954.

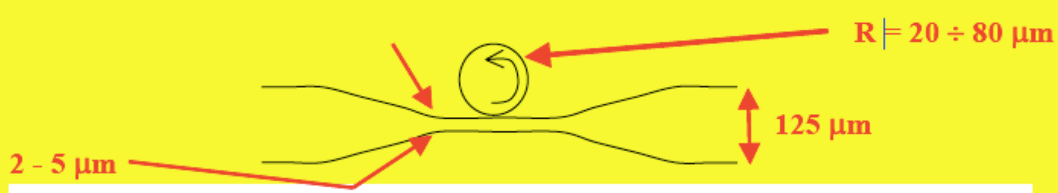

Coupling between a tapered fiber and a microsphere.

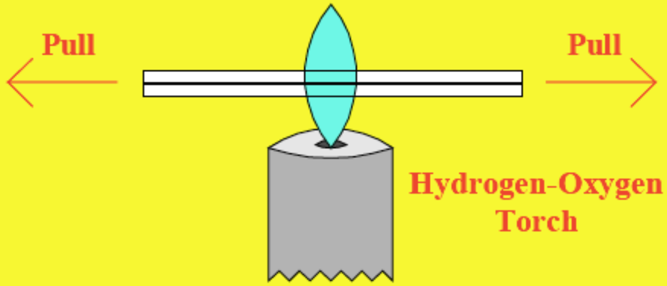

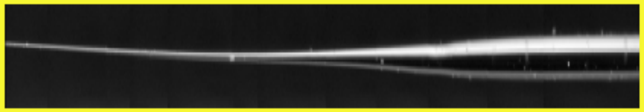

Coupling to a microsphere

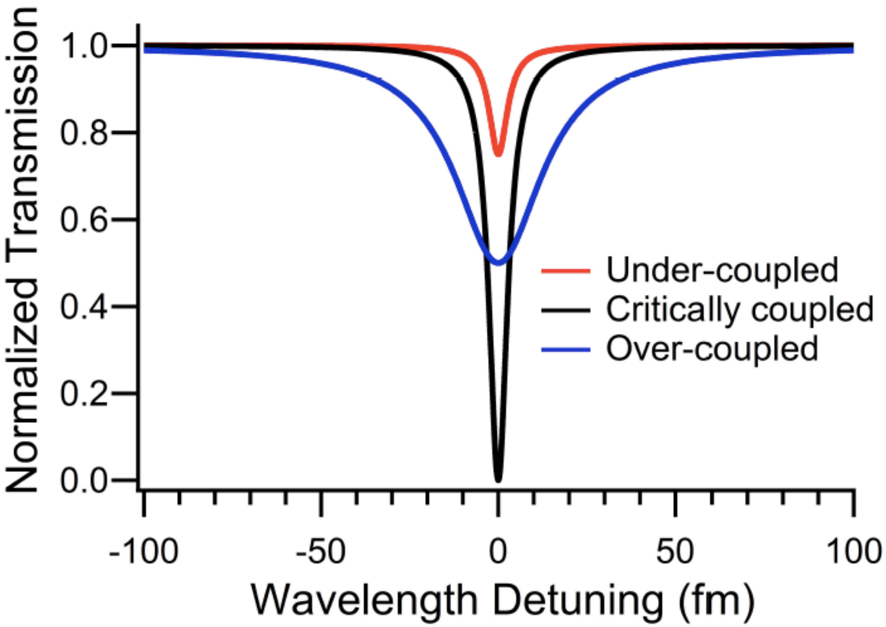

K < 1
K = 1
K > 1

$$T = 1 - [4K / (K + 1)^2]$$

$$K = 1 \Rightarrow T = 0$$

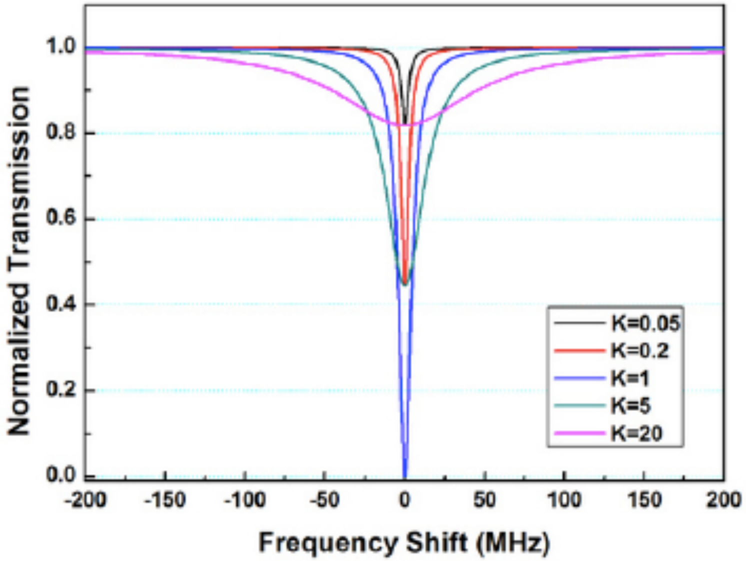

The coupling efficiency can be tuned by controlling the distance between fiber and resonator.

Figure 3.8: The normalized transmission spectrum of different coupling conditions as scanning the frequency of the light. The output transmission becomes zero at resonant frequency only under the critical coupling condition. When the normalized coupling parameter gets away from the unit, the transmission dips are weaker. The dips become narrower in the under coupling region, while in the over coupling region, the dips broaden.

Measurement set-up

Laser Source: *Tunics Plus* tunable laser
operating around 1550 nm

- *$\delta\nu$=300 KHz* (linewidth)
- *$\Delta\nu$= 1.5 GHz* (laser line sweep)
- *< 1 KHz freq. mod*

Detector: *InGaAs*

- ***Thorlabs PDA 400*** (10 MHz bandwidth) for slow scanning;

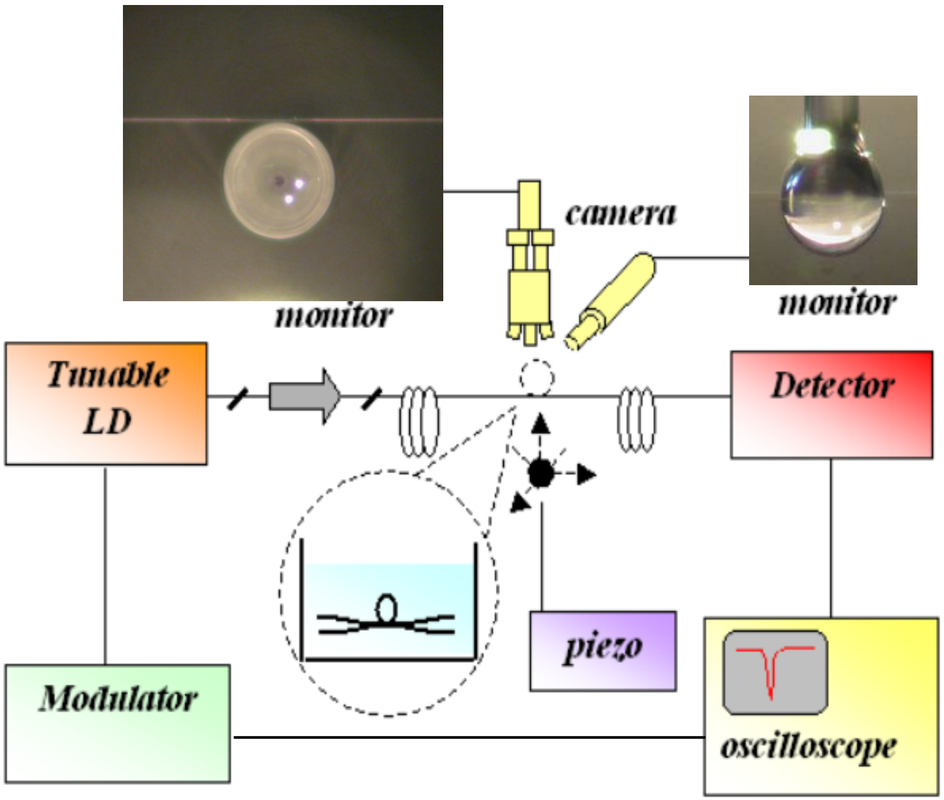

From WGM spectral linewidth *$d\nu$*

$Q=\nu/d\nu$

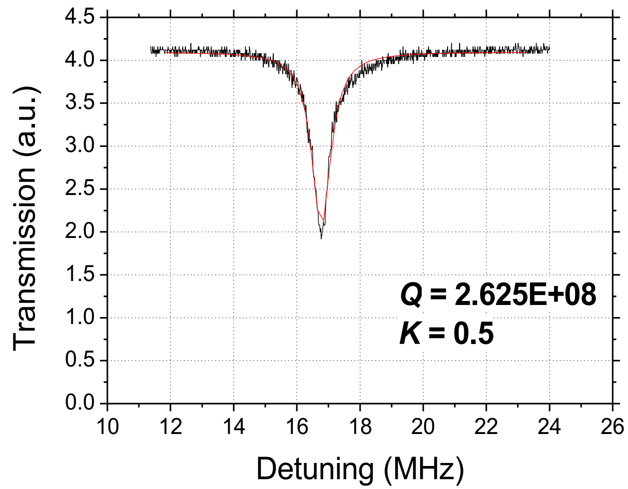

Bulk or hollow structures ?

BULK structures

- Microsphere

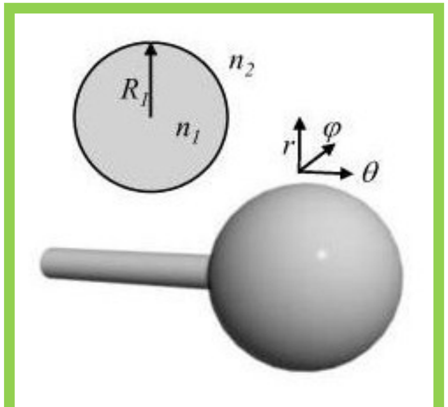

- Microbottle

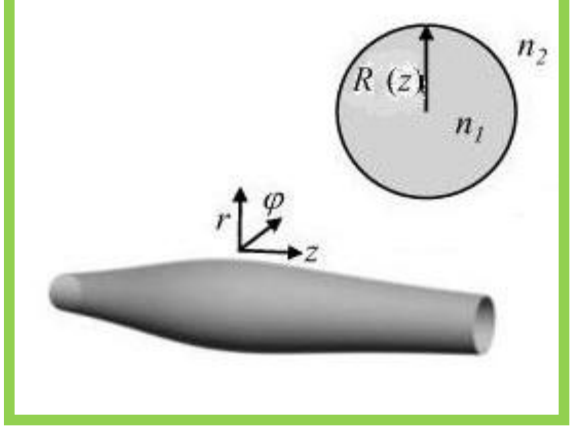

HOLLOW structures

- Capillary

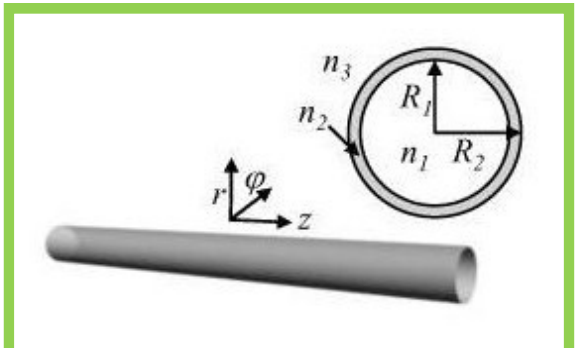

- Microbubble

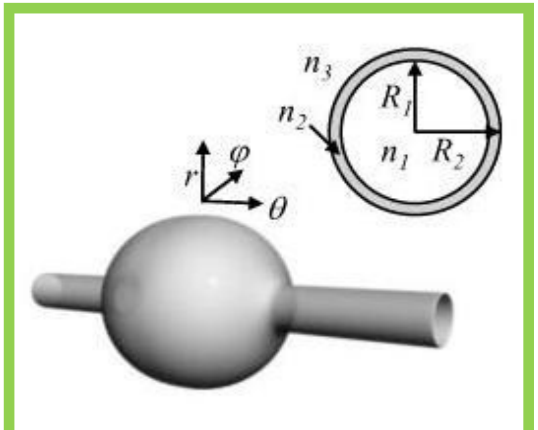

Microbubble Fabrication Method

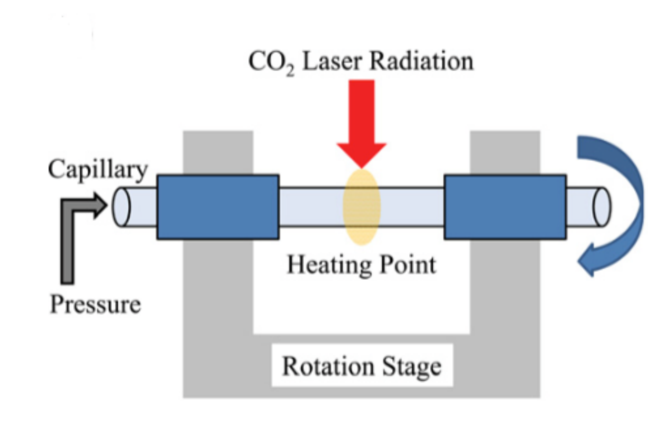

W. Lee *et al.*, Appl. Phys. Lett. 99, 091102 (2011)

Our approach: steady capillary + arc discharge between the rotating splicer electrodes

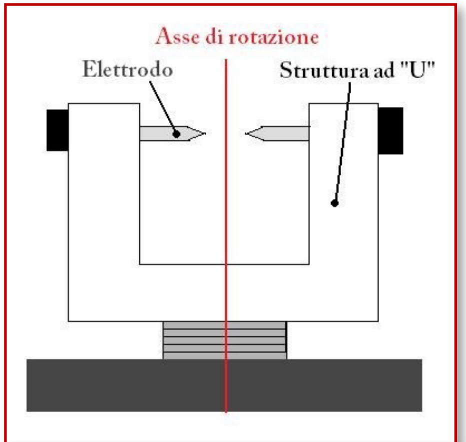

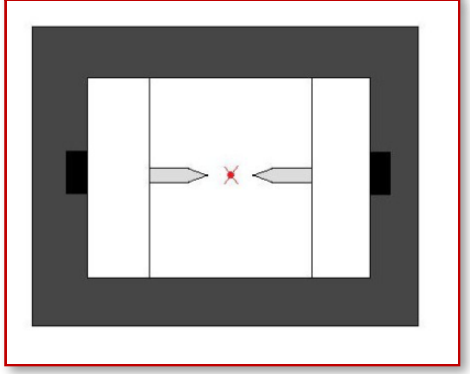

Capillary
⬇
Microbubble

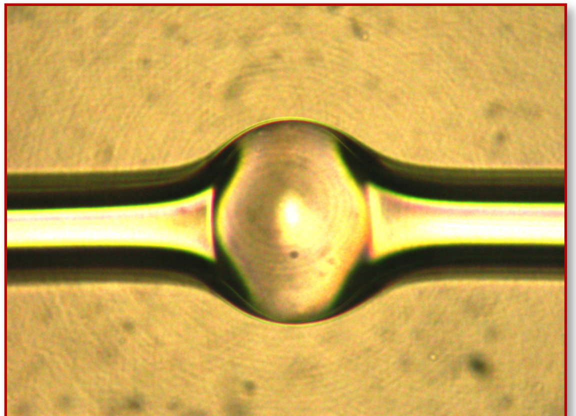

D_c= 280 µm S_c=20 µm

⬇

D_b= 380 µm S_b=4 µm

Q = 1.7 x 10^7

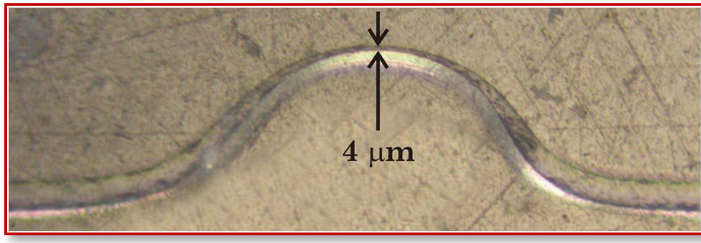

Fabrication Improvement

Two parallel arc discharges (4 electrodes) have been used to produce a uniform heating volume around the capillary

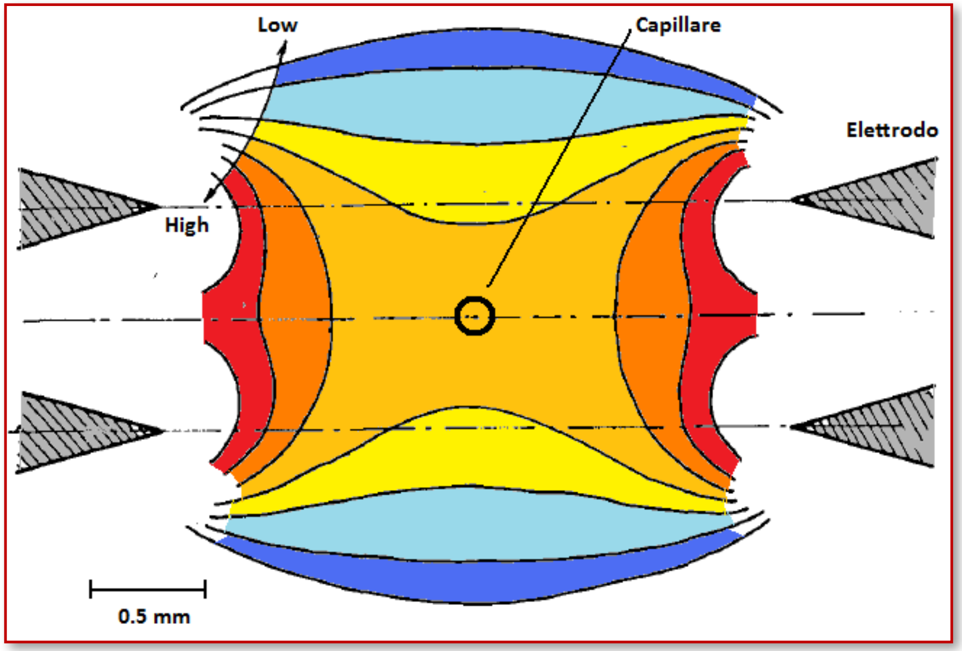

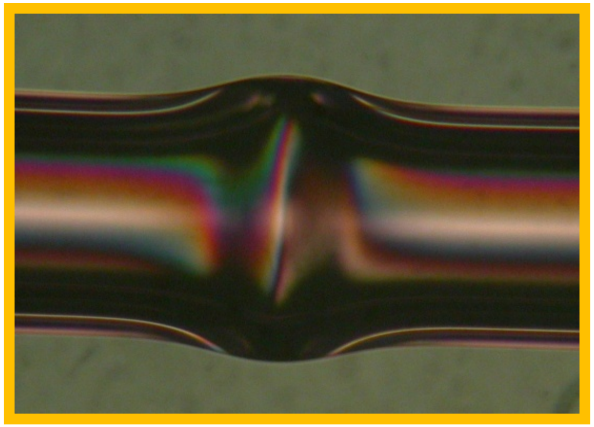

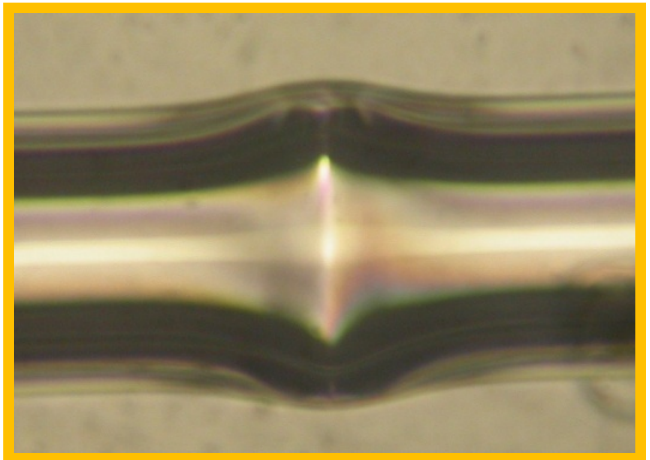

Microbubble Fabrication (set-up)

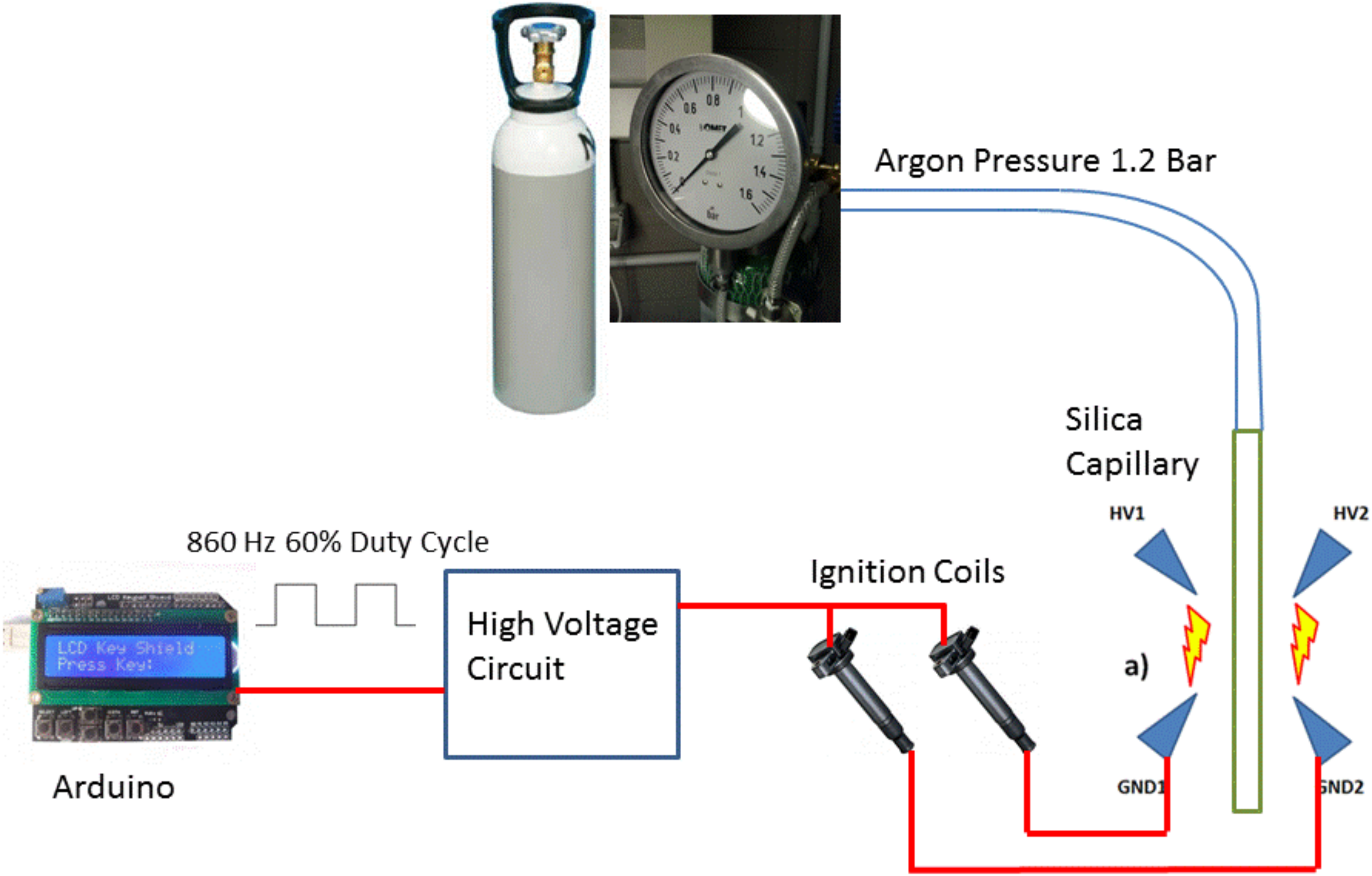

Microbubble Fabrication (exp.)

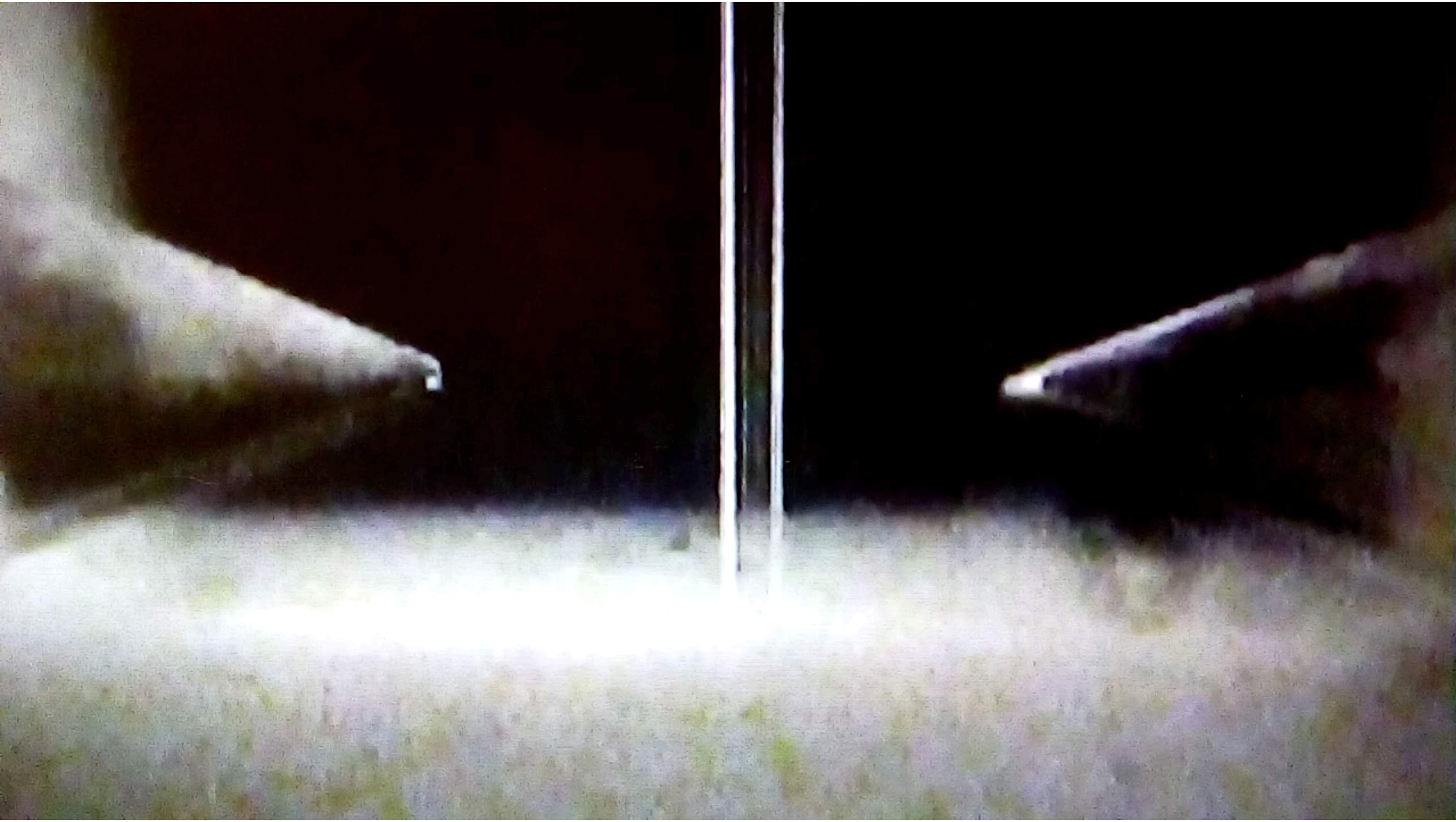

Microbubble Characterization

The thickness of the wall is critical to get highly efficient interaction with the liquid flowing inside. We developed a non-destructive measurement technique by using confocal microscopy.

A. Cosci, F. Quercioli, D. Farnesi, S. Berneschi, A. Giannetti, F.. Cosi, A. Barucci, G. Nunzi Conti, G. Righini, and S. Pelli, "Confocal reflectance microscopy for determination of microbubble resonator thickness," Opt. Express 23, 16693 (2015)

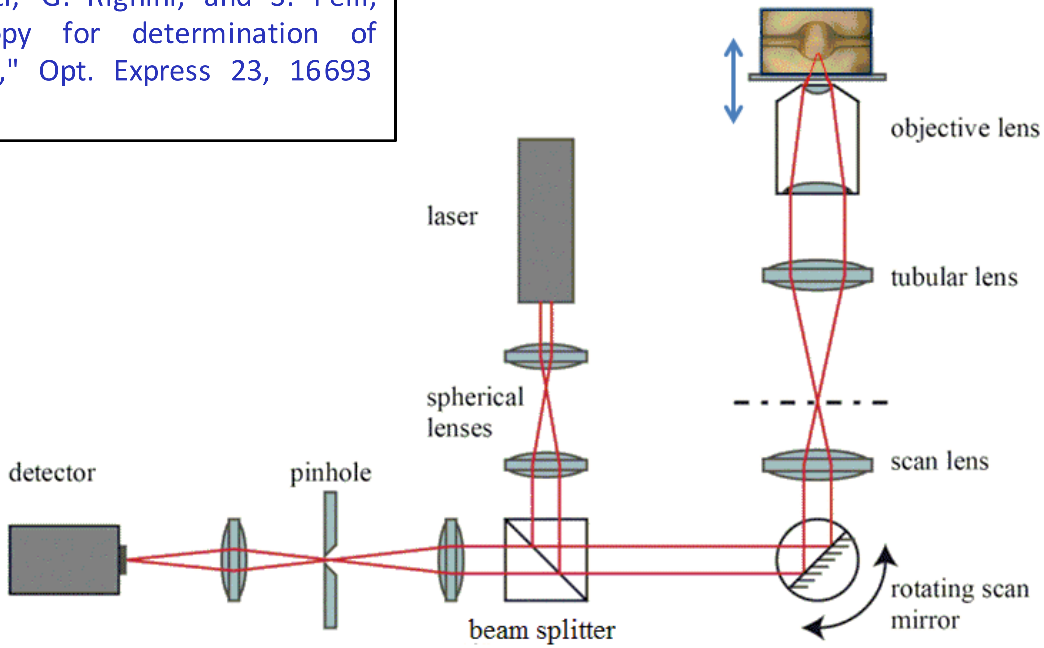

Confocal measurement

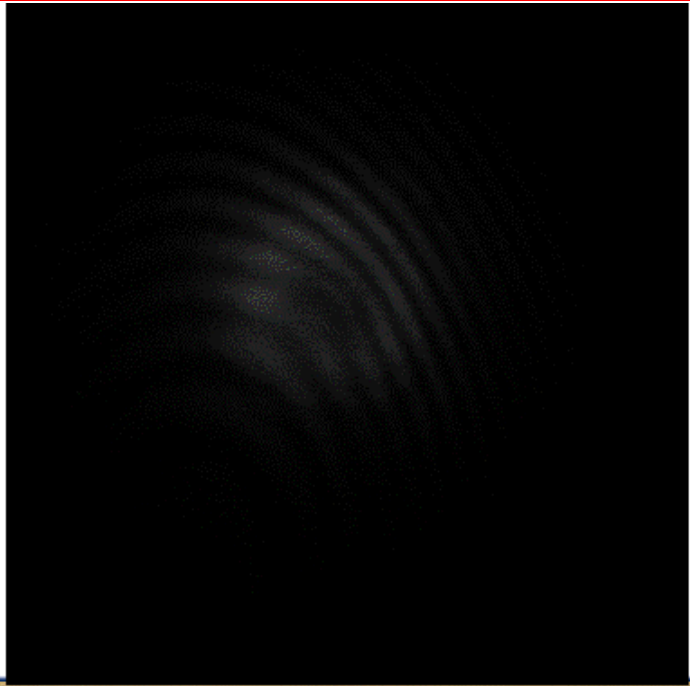

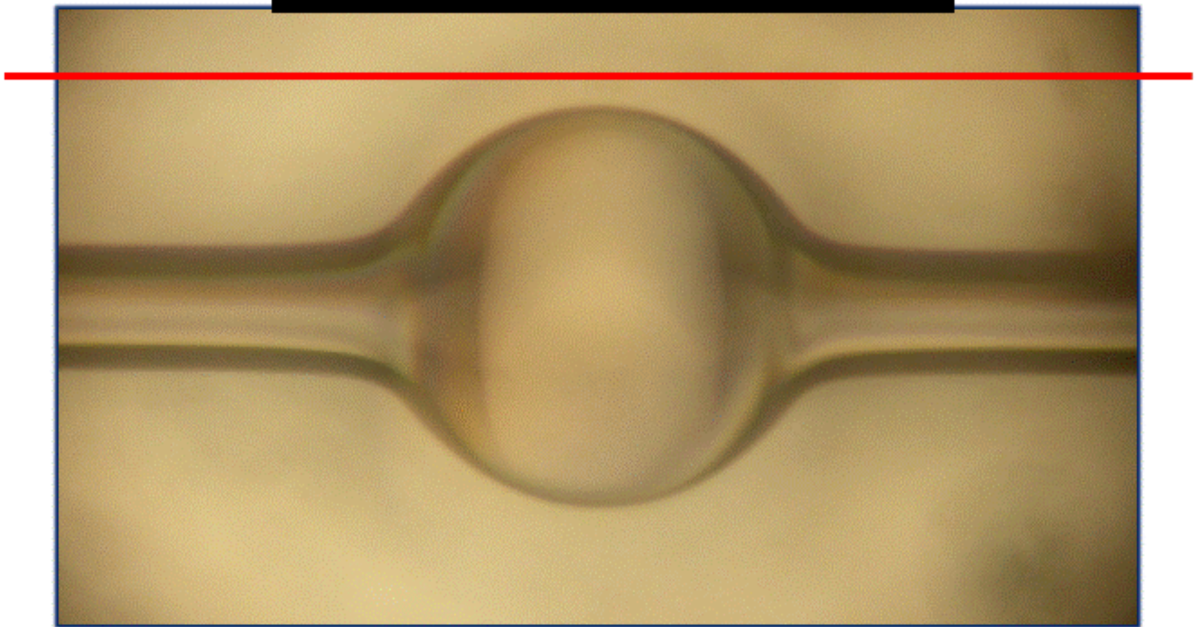

Lasing in Spherical Microresonators

WGMR Lasers

Spherical WGMRs offer very simple routes to the development of microlasers, e.g.:

a) use either an active material for the fabrication of the microsphere or an active coating on a silica microsphere. Oxide glasses doped with rare earth ions are excellent active materials. By exploiting nonlinear effects, however, other materials such as As_2S_3 can be used to produce Raman lasers.

b) use a liquid dye in a microbubble resonator.

WGMR Lasers - History

The pioneer work in this area dates back to 1961, when Garrett *et al.* published a paper in Phys. Rev. on stimulated emission in Sm^{++} doped CaF_2 spheres.

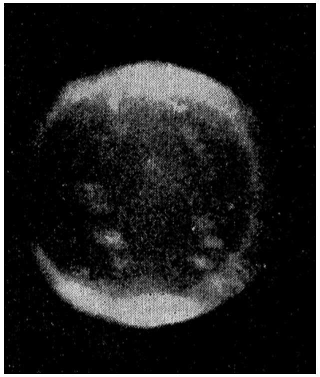

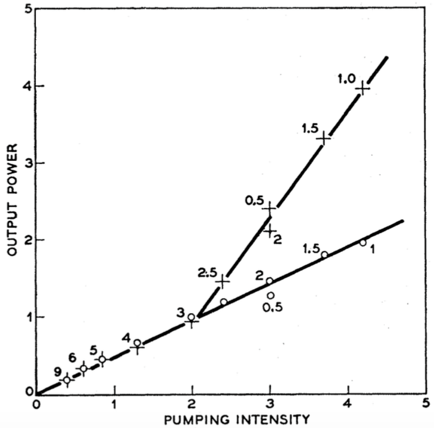

Fig. 3. Dependence on pumping intensity of the emission from the disk (circles) and from the rim (crosses). Numbers indicate intervals of time from the beginning of the flash in microseconds.

1 < 2R < 2 mm

in liquid hydrogen

Pumped by a flashlamp

We believe that these observations, and especially the existence of a sharp threshold (see Fig. 3), indicate that maser action is taking place.

Next step was the observation of lasing in dye droplets.

H.M. Tzeng *et al., Opt. Lett. 9, 499 (1984)*

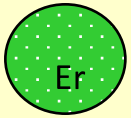

Active Medium
+
Resonant Cavity

Fiber-coupled microsphere laser

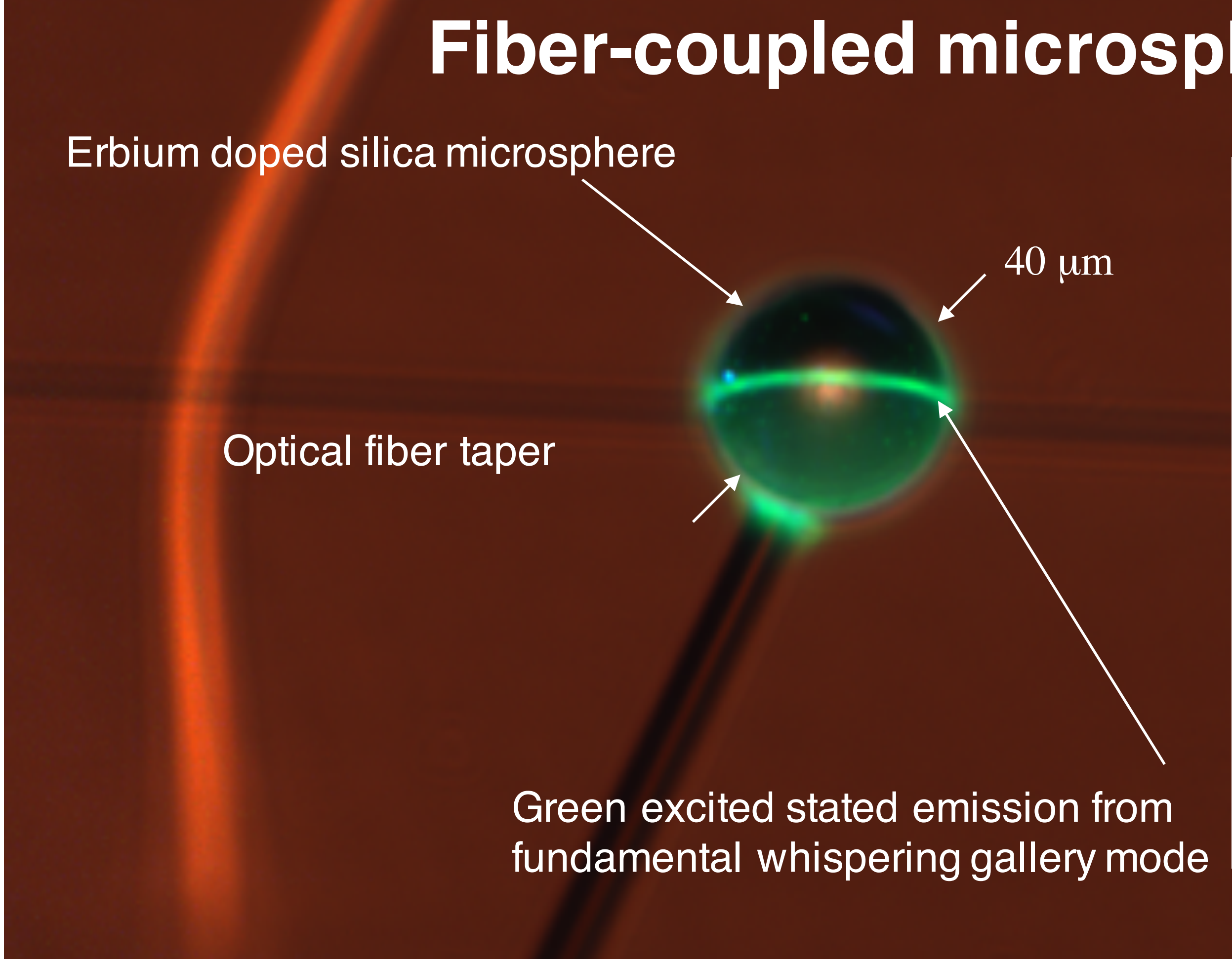

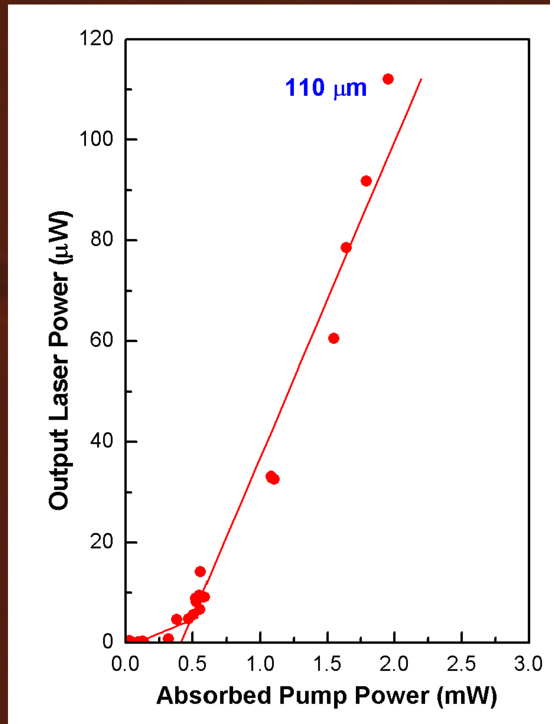

Micro-cavity laser (Vahala group)
US Patent 6741628 B2 (priority date 9 March 2000)

Image credit: Kerry Vahala

WGMR lasers

Er^{3+}-doped ZBLAN glass (0.2 wt%)

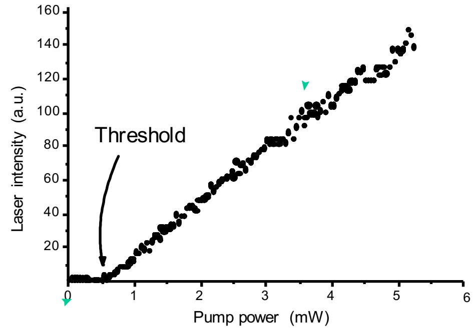

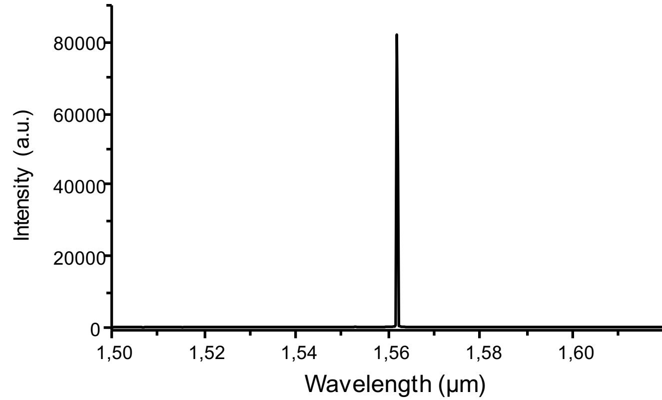

ZBLAN is a composite glass (ZrF4, BaF2, LaF3, AlF3 and NaF), exhibiting wide transmission wavelength range (0.35µm ~ 4µm).

G. Nunzi Conti *et al.*, J. Non-Cryst. Solids 352, 2360 (2006)

D. Ristic *et al.*, J. Luminescence 170, 755 (2016)

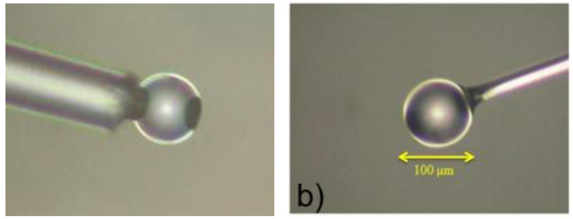

Fig.1. Optical image of: a) a microsphere of about 80 µm fabricated by direct melting of glass powder and glued to the tip of a fiber; b) a 'monolithic' microsphere fabricated directly from the tip of an Er^{3+} doped phosphate glass thread.

Er^{3+}-$Yb3^{+}$ Schott IOG-2 glass (2 wt%)

Phosphate glass

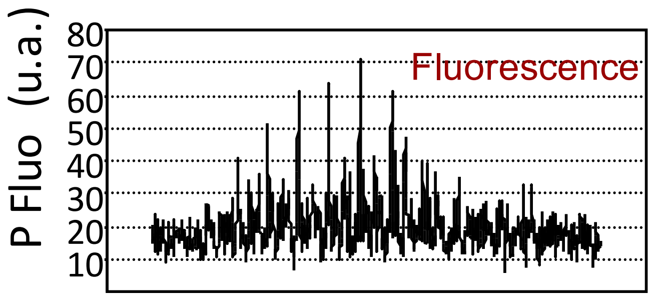

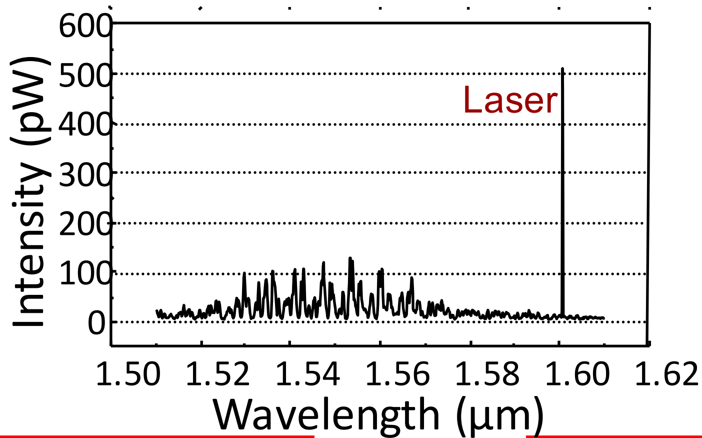

WGMR lasers

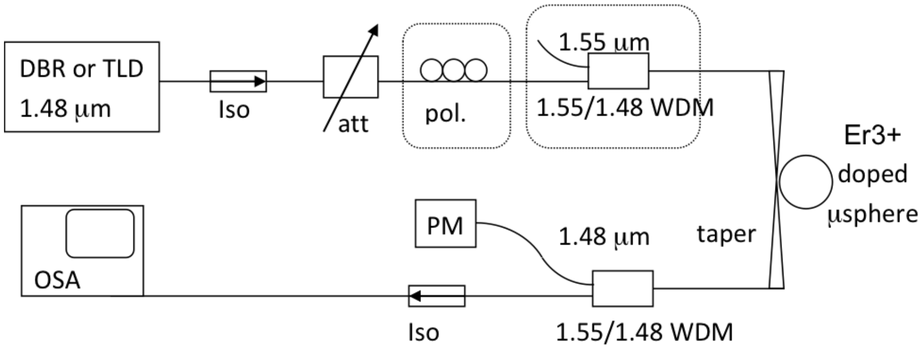

glass	τ_{meas} (± 0.2 ms)	τ_{meas} (± 0.2 ms) sphere	λ *(nm)*	$\Delta\lambda^{eff}_{fl.}$ *(±1 nm)*	σ_{ε} *(±0.01 cm^2)*
IOG10	10.2	6.2	1535	32	5.8×10^{-21}
IOG2	6.8	5.8	1533	50	8×10^{-21}
IOG1	10.7	8.7	1534	30	7×10^{-21}

Er^{3+}-Yb^{3+} Schott IOG-1 glass
75 μm microsphere
Record 90 μW @ 1568.3 nm using a 6.1 mW pump @ 1480 nm

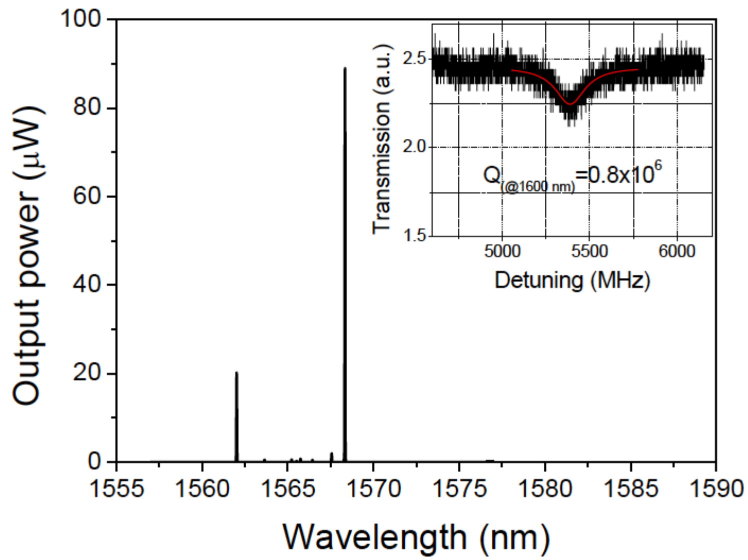

D. Ristic *et al.*, J. Luminescence 170, 755 (2016)

WGMR lasers

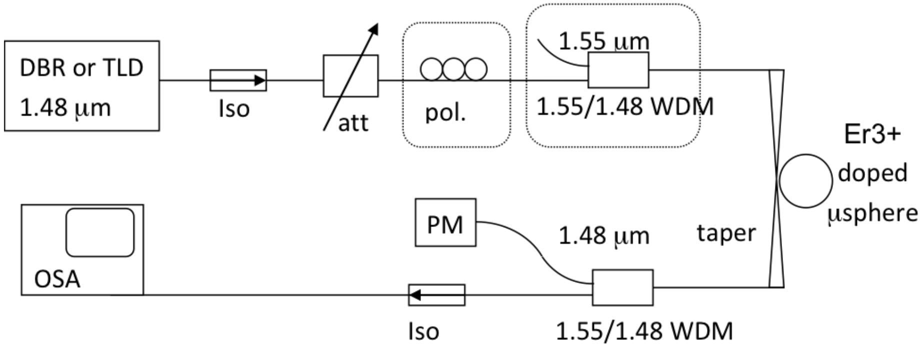

glass	τ_{meas} ($\pm$ 0.2 ms)	τ_{meas} ($\pm$ 0.2 ms) sphere	λ (nm)	$\Delta\lambda^{eff}_{fl.}$ ($\pm$1 nm)	σ_{ε} ($\pm$0.01 cm^2)
IOG10	10.2	6.2	1535	32	5.8×10^{-21}
IOG2	6.8	5.8	1533	50	8×10^{-21}
IOG1	10.7	8.7	1534	30	7×10^{-21}

Er^{3+}-Yb^{3+} Schott IOG-1 glass

75 μm microsphere

Record 90 μW @ 1568.3 nm using a 6.1 mW pump @ 1480 nm

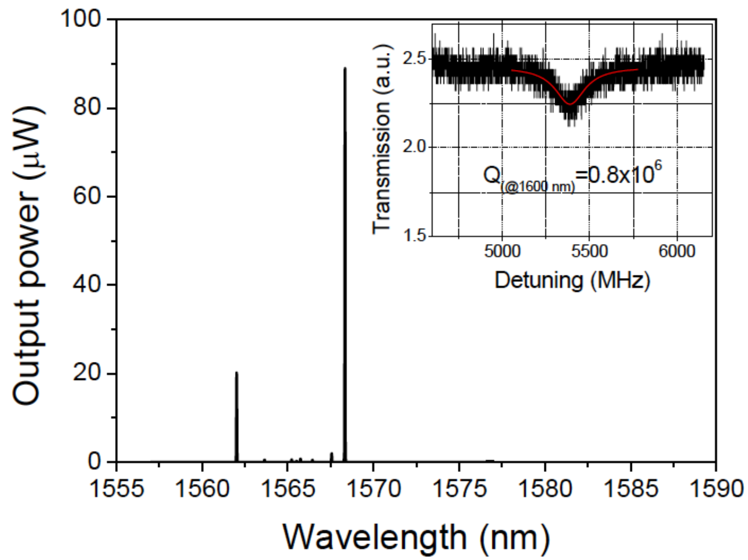

D. Ristic *et al.*, J. Luminescence 170, 755 (2016)

Active coating of a WGMR

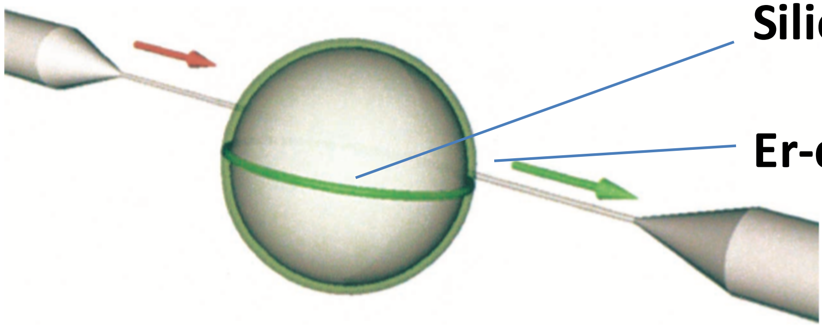

Silica microsphere 50 < 2R < 80 μm

Er-doped silica sol-gel coating 1 < d < 20 μm

300 nm-thick 70 SiO_2-30HfO_2 film activated with 1% mol of Er^{3+}

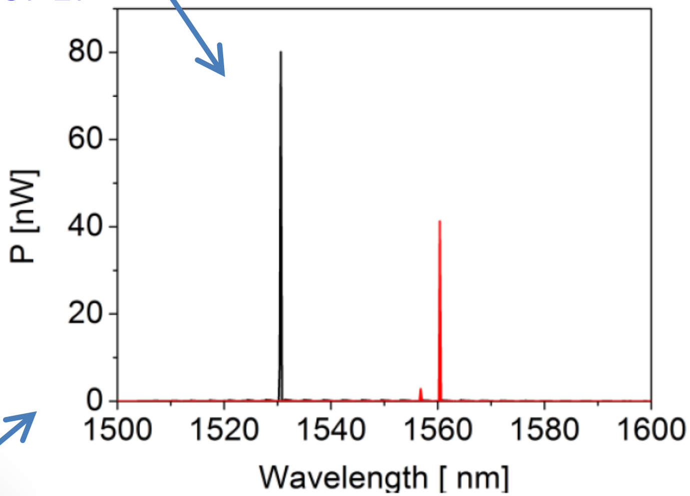

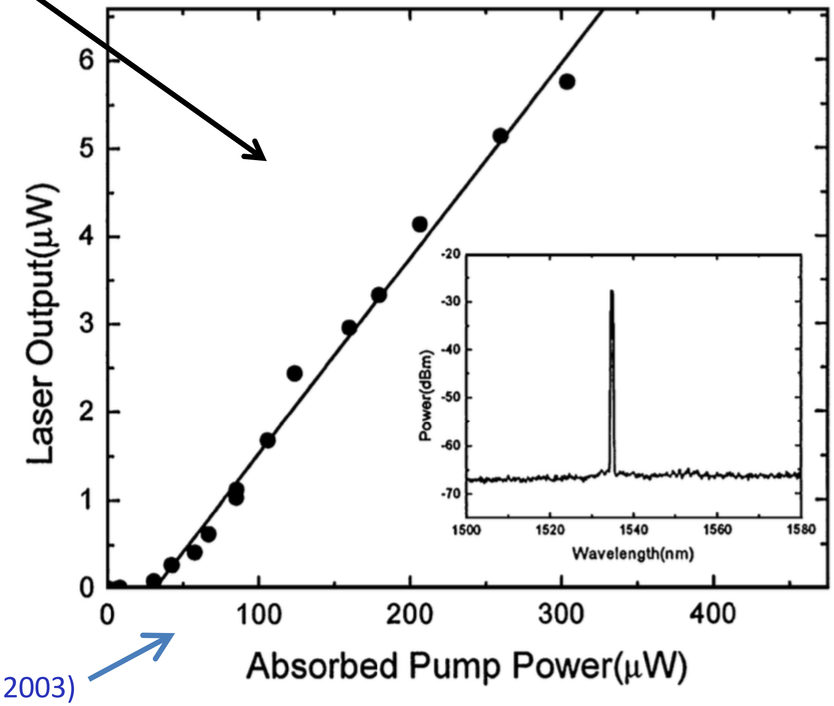

L. Yang and K.J. Vahala, Opt. Lett. 28, 592 (2003)

D. Ristic *et al.*, J. Luminescence 170, 755 (2016)

Coating by quantum dots

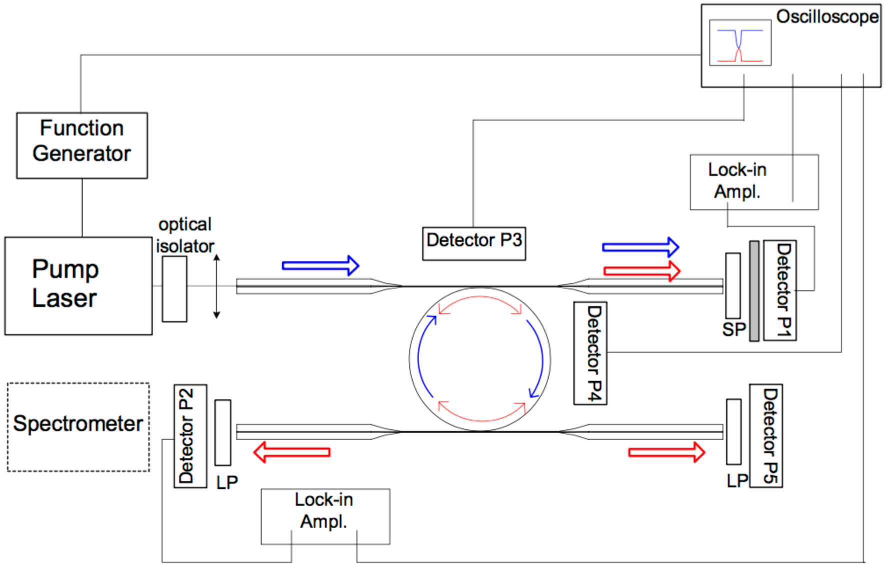

Silica microsphere 100 < 2R < 1000 μm

HgTe / HgCdTe quantum dots (2R = 3 – 4 nm) on the sphere's surface.

Laser pump @ 830 nm

Laser emission in the 1240 to 1780 nm range

Threshold pump power 480 nW.

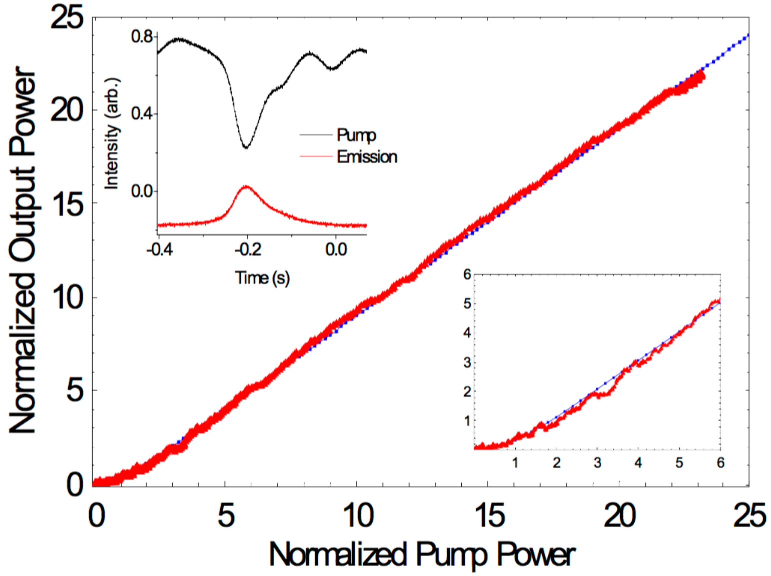

Fig. 2. Fit of results to model. Upper inset: simultaneous traces of pump throughput dip and emission peak. Lower inset: detail of behavior in the vicinity of threshold.

S. I. Shopova *et al.*, Appl. Phys. Lett. 85, 6101 (2004)
S. I. Shopova *et al.*, *Proc. OSA/CQO, CsuA19* (2007)

Microbubble dye laser

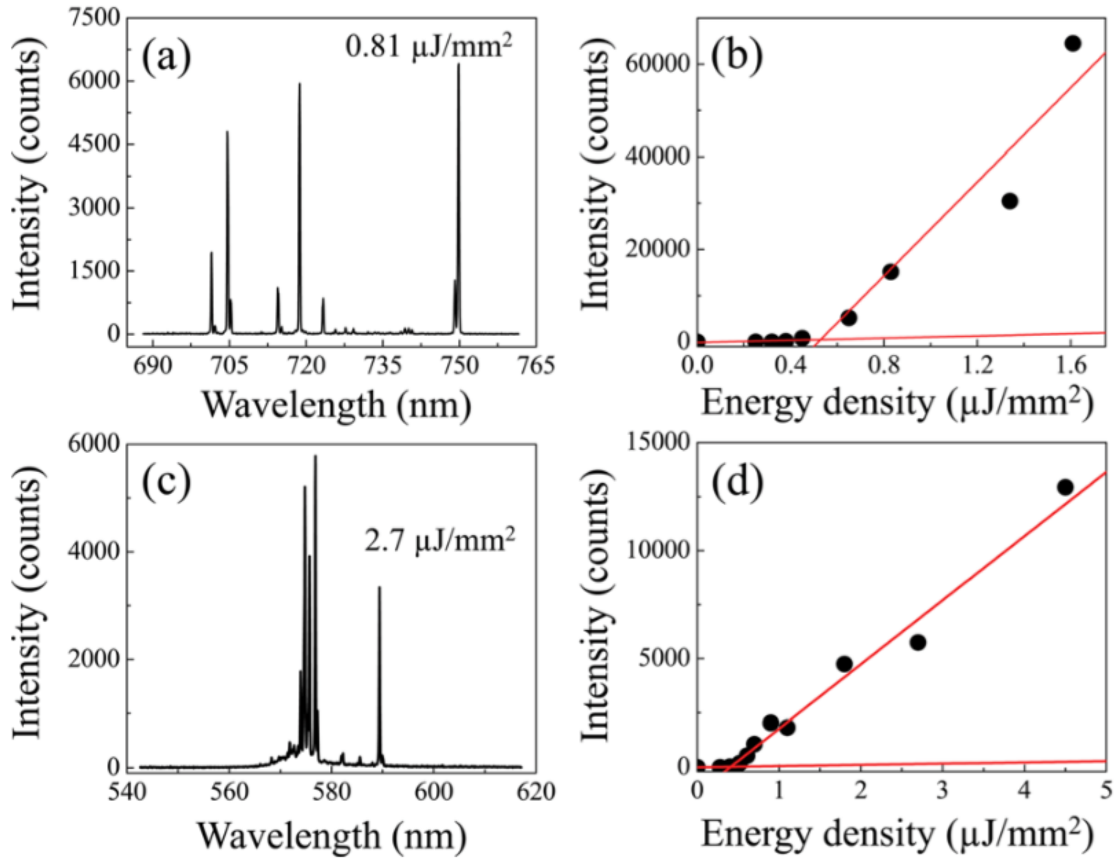

W. Lee *et al.*, A quasi-droplet optofluidic ring resonator laser using a micro-bubble, Appl. Phys. Lett. 99, 091102 (2011)

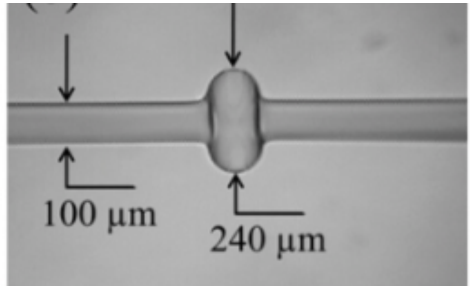

0.6 < wall thickness < 4.5 μm

$Q > 10^6$

The micro-bubble is pumped by a 5 ns pulsed optical parametric oscillator at 532 nm.

(a) 1 mM LDS722 dye dissolved in methanol; (b) threshold curve; P_{th}= 0.52 μJ/mm².

(c) 1 mM R6G dye dissolved in quinoline; (d) threshold curve; P_{th}= 400 nJ/mm².

Polymeric microbottle laser

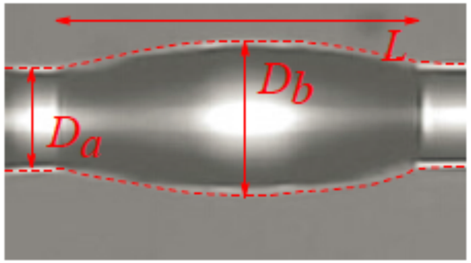

0.3 wt% of Rh.B dissolved into SU-8 polymer matrix

D_b = 230 μm, D_a = 125 μm, L_b = 690 μm

SHG-Nd:YAG laser (532 nm, 30 ps pulse width) pump light.

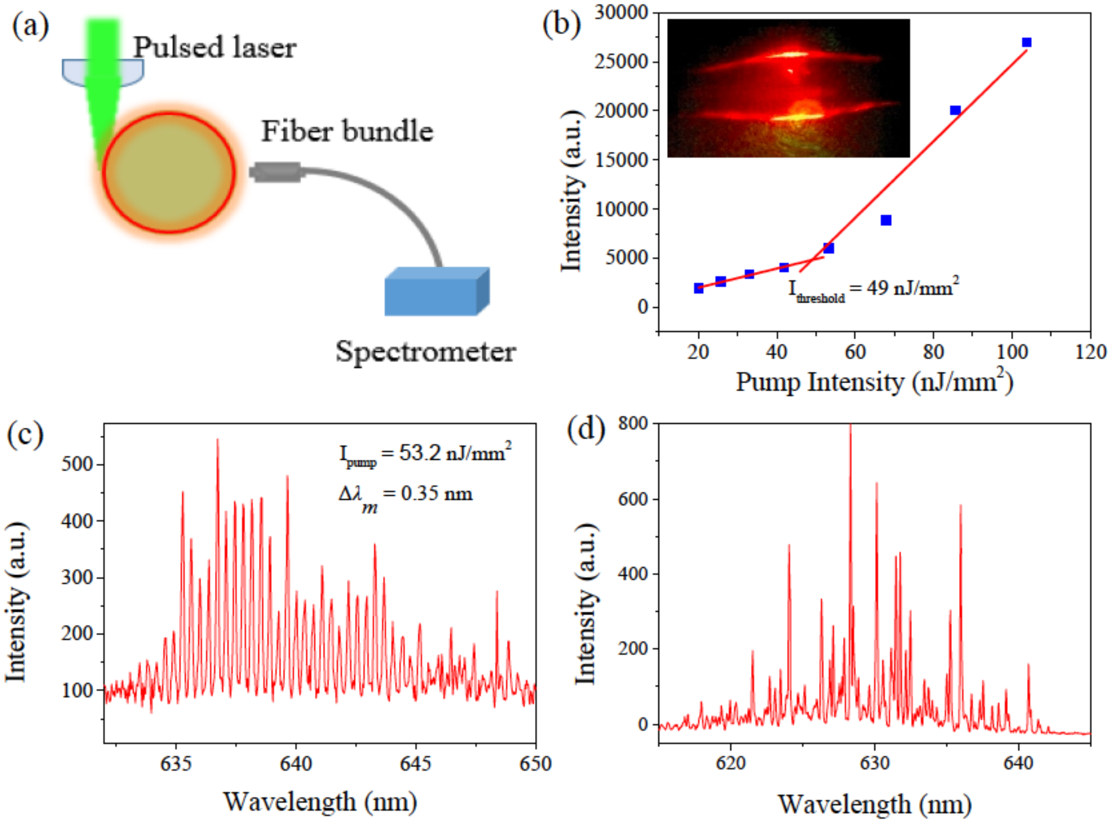

Q. Lu *et al.*, Mode-selective lasing in high-Q polymer microbottle resonators, Opt. Exp. 23, 22740 (2015)

Raman laser

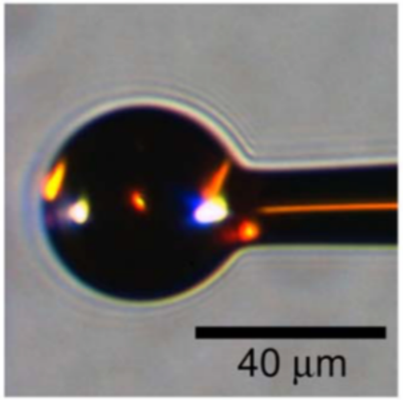

Microspheres are fabricated by CO_2 laser reflow process applied to a high purity As_2S_3 fiber.

$10^6 < Q < 10^8$

Raman gain $g_R \sim 4.4 \times 10^{-10}$ cm/W

Pump tunable laser is scanned around a central wavelength of 1549 nm. The SRS emission is expected to be shifted 10.3 THz away from the pump and to be around 1635 nm.

A microsphere with a diameter of 71 µm is used.

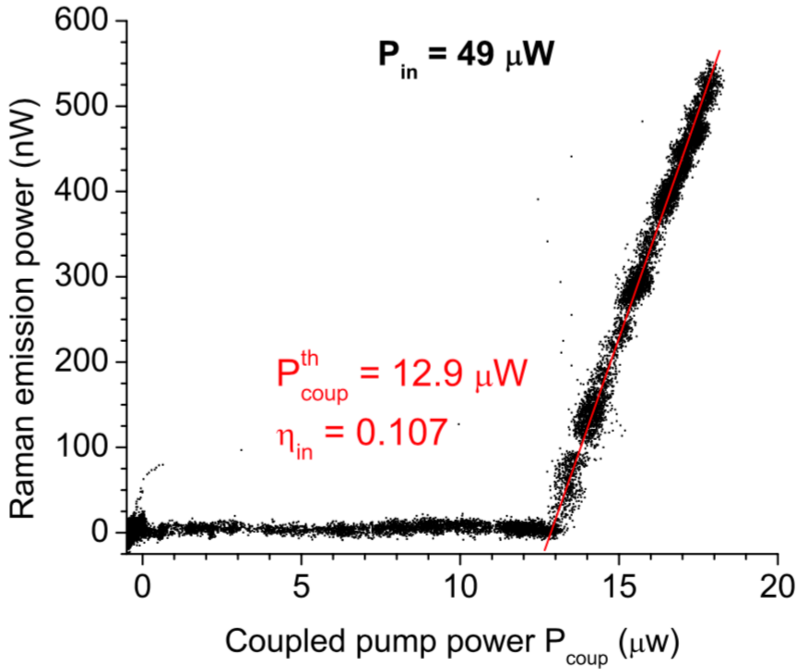

F. Vanier *et al.,* Opt. Lett. 38, 4966 (2013)

Nonlinear Optics in Spherical Microresonators

NLO in silica or hybrid WGMRs

Even if silica exhibits relatively modest nonlinear coefficients, the ultra-high-Q WGMRs have found use for nonlinear applications including all-optical switching and third harmonic generation.

Bulk silica glass, being centrosymmetric, cannot possess any second order nonlinearity. A coating with radially aligned nonlinear molecules, however, is sufficient to permit 2nd-order parametric processes. [Y. Xu *et al.*, PRL 100, 163905 (2008)]

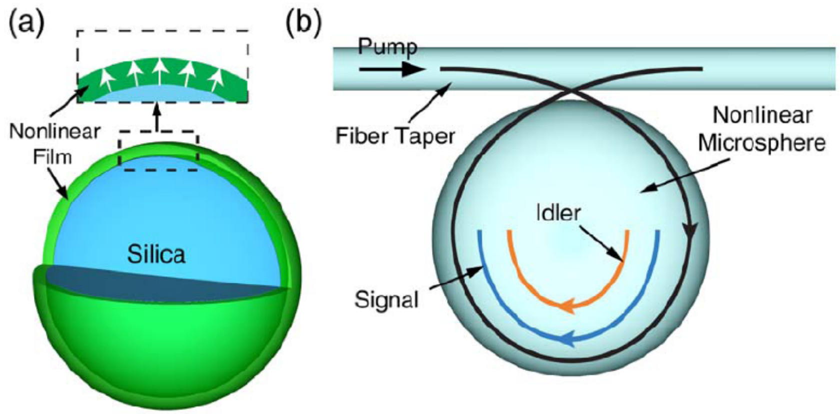

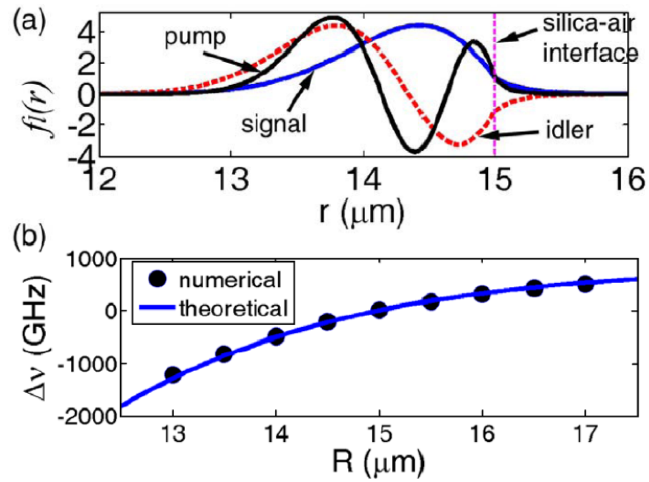

Since silica microspheres possess a large number of high-Q WG modes, satisfying both the on-resonance condition and the requirement of angular momentum conservation is not difficult. For a microsphere with a radius of 15 μm, nonlinear layer thickness of 50 nm, and Q = 5 10^6, an ultra-low threshold of parametric oscillation equal to 78 μW was calculated.

Third order NLO in SiO_2

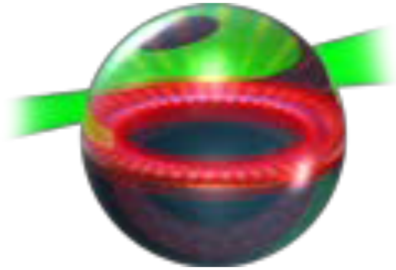

Phil Saunders/spacechannel.org

Raman Scattering $\Delta\upsilon_R$= 10 THz, g_R
(interaction with an optical phonon)

Brillouin Scattering $\Delta\upsilon_B$= 17MHz, g_B= 500 g_R
(interaction with an acoustic phonon)

Four Wave Mixing: hyperparametric interaction g_P= 2 g_R

Pure gain processes, such as stimulated Brillouin scattering (SBS) and stimulated Raman scattering (SRS), are automatically phase matched. SRS is the easiest to generate and often competes with optical (hyper)-parametric oscillations, such as four-wave-mixing (FWM), which has a higher gain but stringent phase matching conditions.

D. Farnesi, A.Barucci, G.C. Righini, S. Berneschi, S. Soria, and G. Nunzi Conti, Optical frequency conversion in silica whispering gallery mode microspherical resonators", Phys. Rev. Lett. 112 , 093901 (2014)

Hyperparametrical Interactions

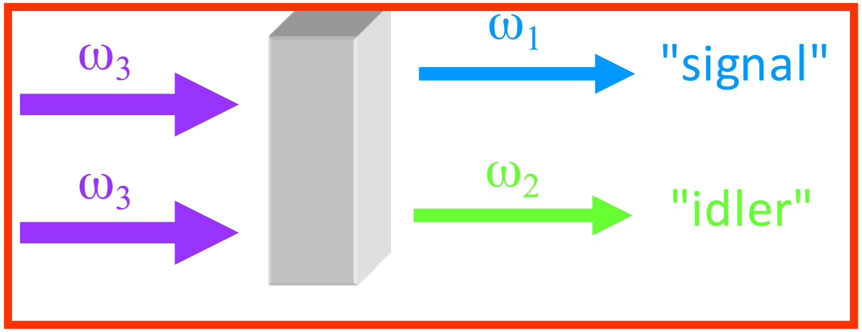

$$n = n_0 + n_2 I$$

$$P^{(3)} = \varepsilon_0 \chi^{(3)} E_1 E_2^* E_3$$

$$2\,\omega_p = \omega_s + \omega_i$$

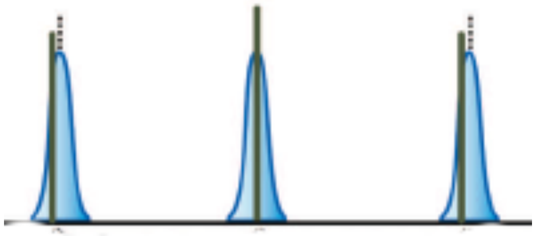

Cross Phase Modulation (XPM)
and Self Phase Modulation (SPM) pull the modes into resonance

$$2\,\beta_m = \beta_{m-n} + \beta_{m+n}$$

Intrinsically satisfied for WGM with angular mode simmetrically spaced

Experimental setup

4508 Vol. 40, No. 19 / October 1 2015 / Optics Letters Letter

Optics Letters

Generation of hyper-parametric oscillations in silica microbubbles

Daniele Farnesi,[1,2] Andrea Barucci,[1] Giancarlo C. Righini,[1,2] Gualtiero Nunzi Conti,[1] and Silvia Soria[1,*]

[1]IFAC-CNR, Institute of Applied Physics "N. Carrara," Via Madonna del Piano 10, 50019 Sesto Fiorentino (FI), Italy
[2]Centro Studi e Ricerche "E. Fermi," P. Viminale 2, 00184 Rome, Italy
*Corresponding author: s.soria@ifac.nr.it

Received 7 August 2015; revised 8 September 2015; accepted 8 September 2015; posted 9 September 2015 (Doc. ID 247530); published 29 September 2015

MICROBUBBLE 420 µm < 2R < 475 µm
wall thickness ~ 3 to 4 µm (± 0.5 µm)
Q ~ 3.5 $\times$ 10^7
max P = 80 mW

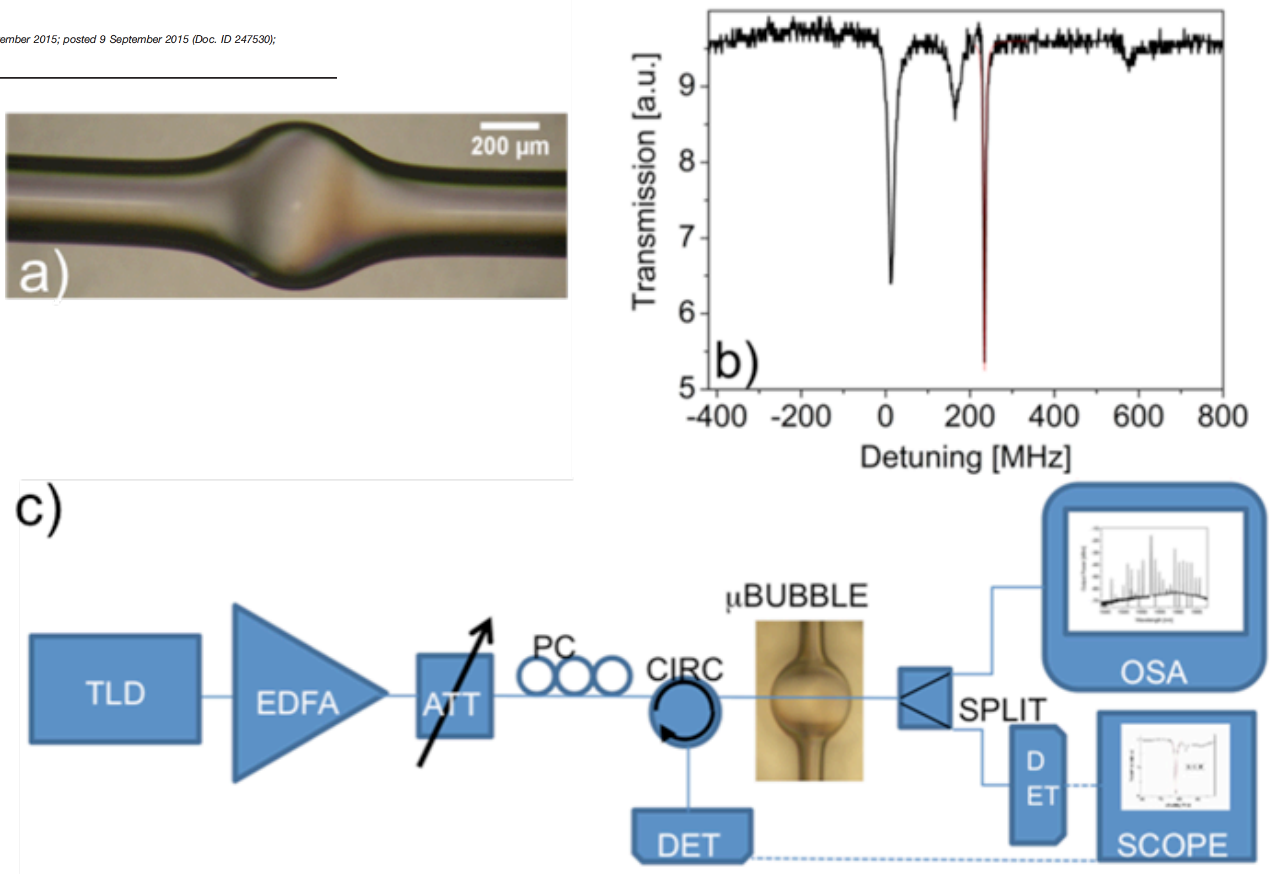

Hyperparametrical Interaction: Four Wave Mixing

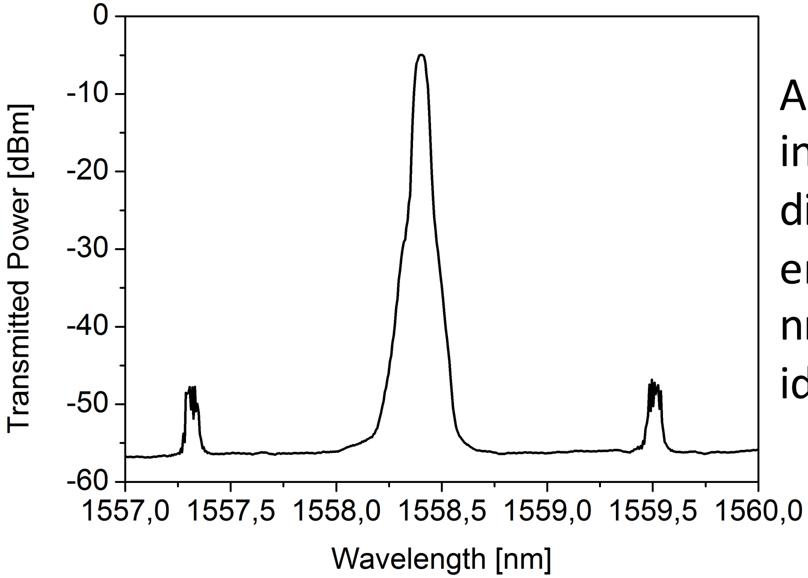

A degenerate FWM of the laser pump (1558,4 nm) in an MBR (2R=475 μm), coupled into the forward direction of the tapered fiber. The idler–signal emission ratio is near unity. The idler is at 1557,3 nm, and the signal at 1559,5 nm. The signal and idler are spaced by twice the free spectral range.

Experimental spectra of a 475 μm diameter MBR with a frequency offset of one FSR.
Inset: spectra of the same microbubble with a frequency offset of 5 FSR.

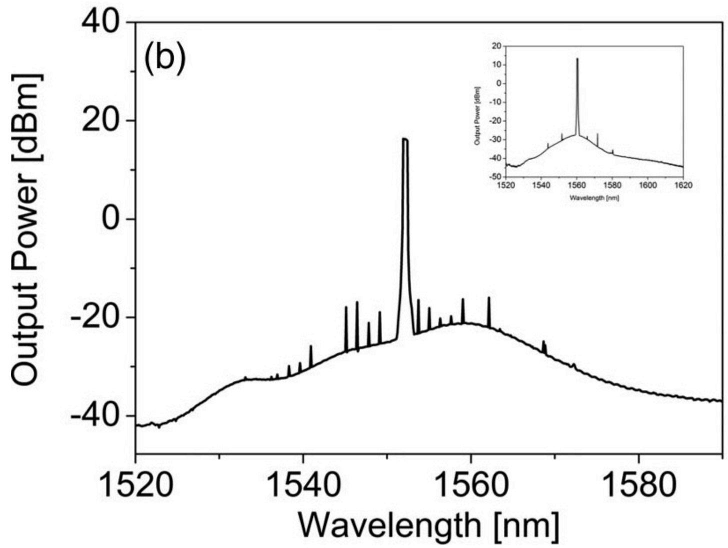

Hyperparametric generation in Silica microbubbles

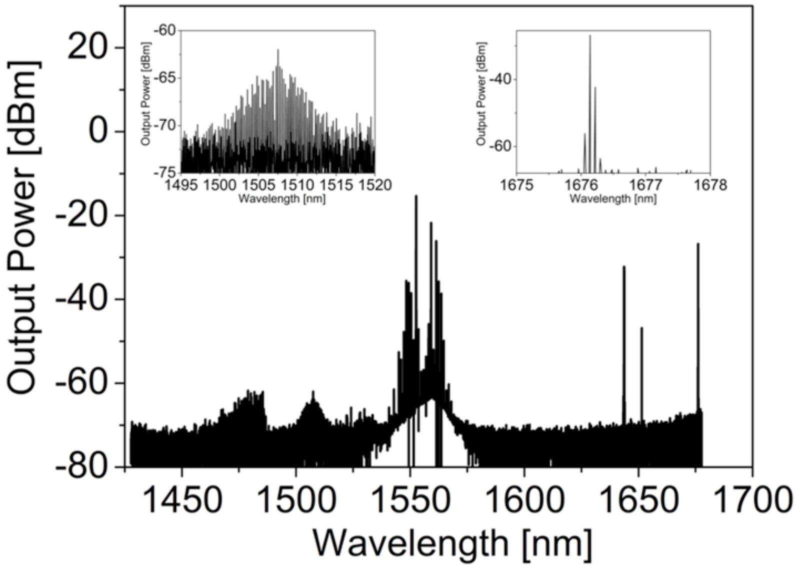

Aperiodic hyper-parametric oscillation with different spacing; FWM in the vicinity of the pump spaced by azimuthal FSR, SRS family modes, and intensity envelope spectrum at anti-Stokes frequency.
Insets: (left) anti-Stokes frequency comb spectrum with a frequency offset of twice the FSR_p (2×0.12 nm), and (right) SRS family modes separated one FSR_p.

Experimental spectrum of a 420 µm MBR showing different SRS lines (in the forward direction). Separation between the pump and the SRS line is ~ 110 nm, which corresponds to the 460 cm^{-1} (13.5 THz) line of the silica Raman gain.

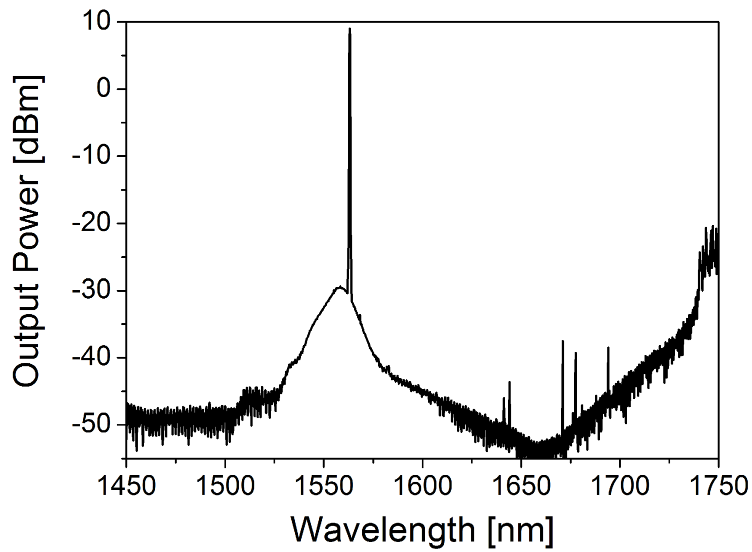

CENTRO FERMI
Museo Storico della Fisica e Centro Studi e Ricerche Enrico Fermi

IFAC

Rainbow laser

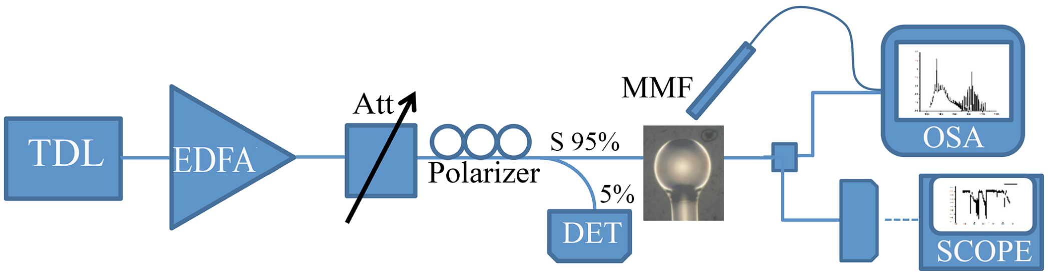

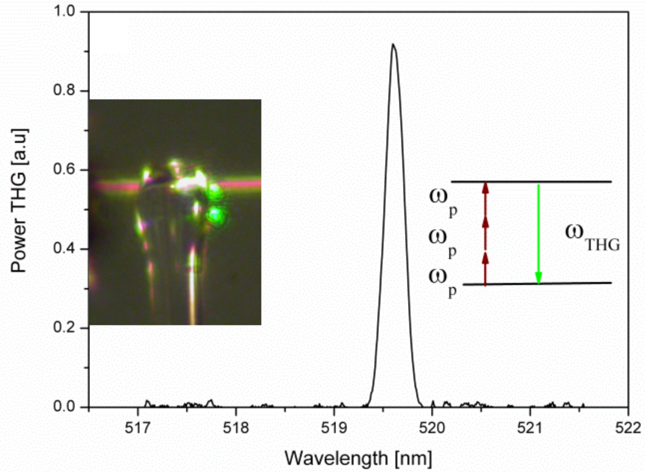

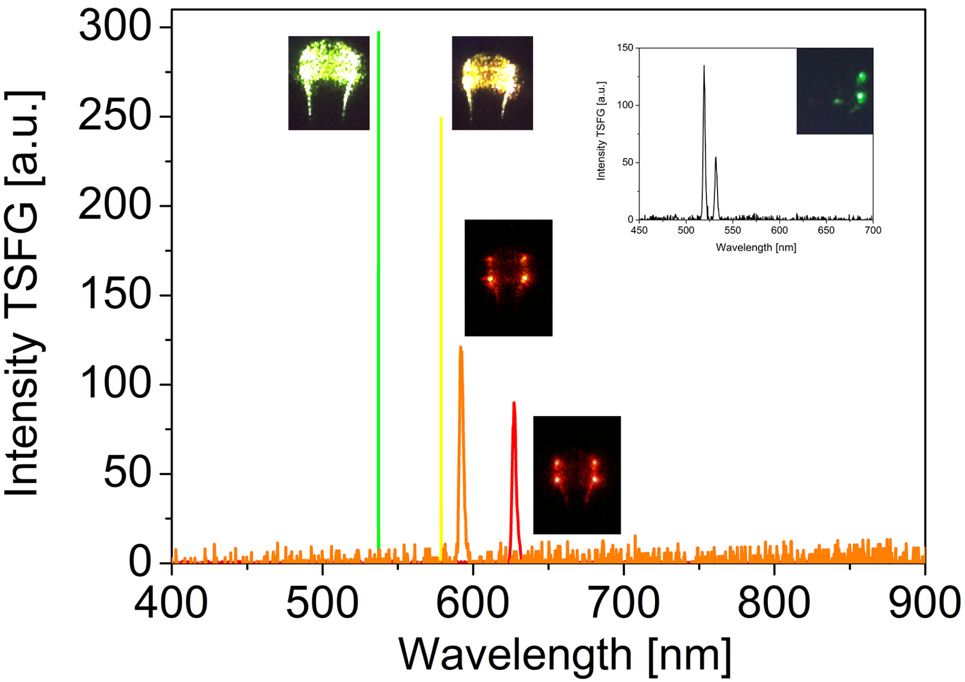

Silica microsphere 2R = 57±1 μm

SRS and TSFG among the Raman lines produce a CW multicolor emission.

Various pump wavelengths within the erbium band gain of the EDFA.

D. Farnesi, A.Barucci, G.C. Righini, S. Berneschi, S. Soria, and G. Nunzi Conti, Multicolour emission in silica whispering gallery mode microspherical resonators, Proc SPIE 8960, 896008 (2014).

CENTRO FERMI Museo Storico della Fisica e Centro Studi e Ricerche Enrico Fermi

IFAC

Biosensing Applications

Applications: WGM sensing

WGMs ARE MORPHOLOGICALLY DEPENDENT IN A VERY SENSITIVE WAY => APPLICATION AS SENSOR

Arnold, Fan, Ilchenko,Vollmer, …

In general, the narrower is the cavity linewidth and:

1) the higher is the Q factor;

2) the higher is the sensor resolution (i. e.: its ability to discriminate the smallest frequency shift that can be accurately measured);

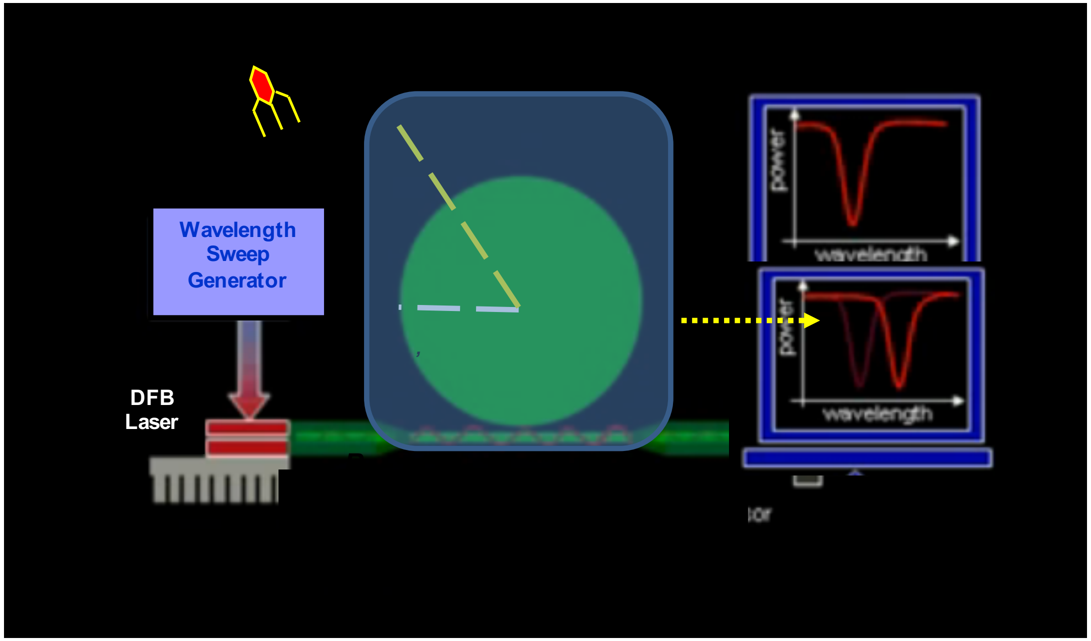

From the resonance condition:

$$\frac{\Delta\lambda_{res}}{\lambda_{res}} = \frac{\Delta r}{r} + \frac{\Delta n}{n}$$

A. Chiasera, Y. Dumeige, P. Féron, M. Ferrari, Y. Jestin, G. Nunzi Conti, S. Pelli, S. Soria, and G. C. Righini, ***Laser Photon. Rev.* 4**, 457 (2010).

Basics of a biosensor

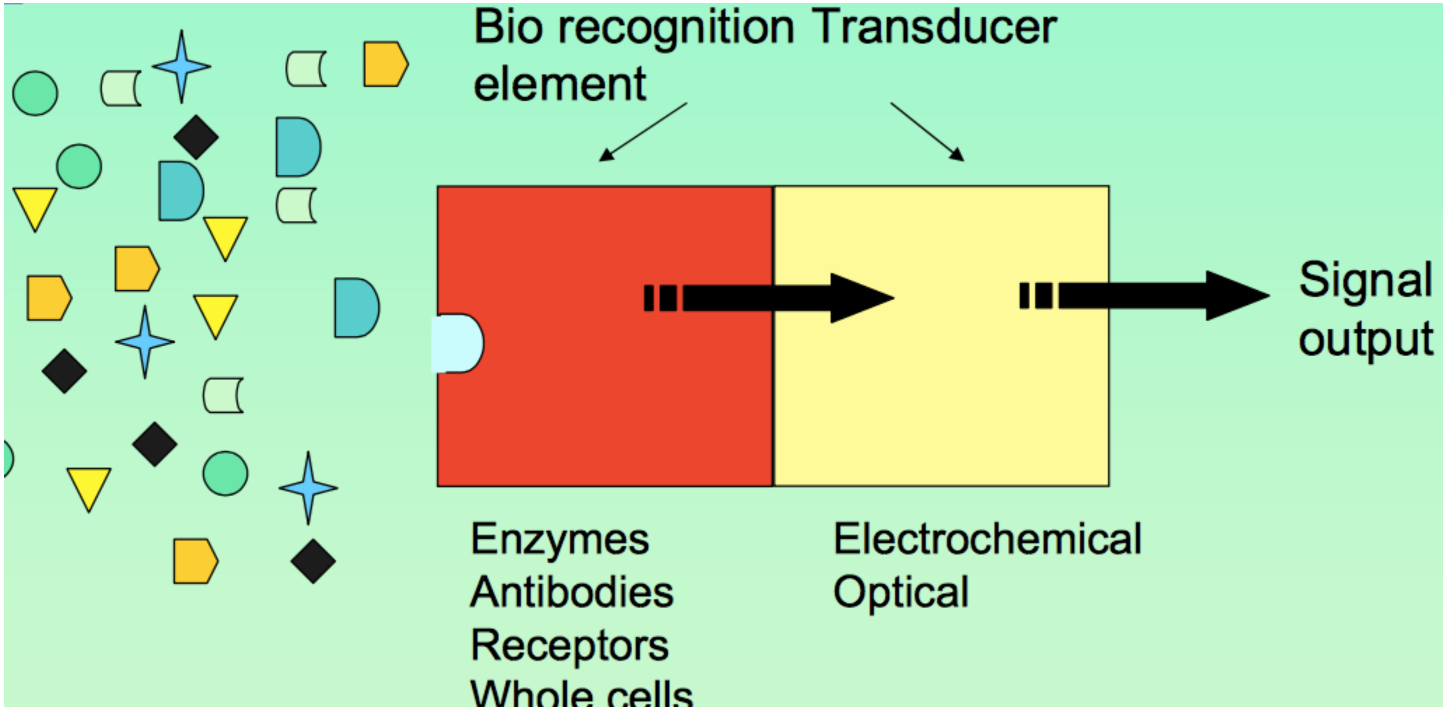

One definition of BIOSENSOR: a device that utilizes biological components, e.g. enzymes, to indicate the amount of a biomaterial"

Biosensing: various binding cases

A crucial issue for **<u>biosensing</u>** is the **selectivity of detection**: it can be achieved by the functionalization of the surface of the microsphere, in order to specifically bind only the biochemical element to be recognized and, at the same time, to maintain a good value for the Q factor.

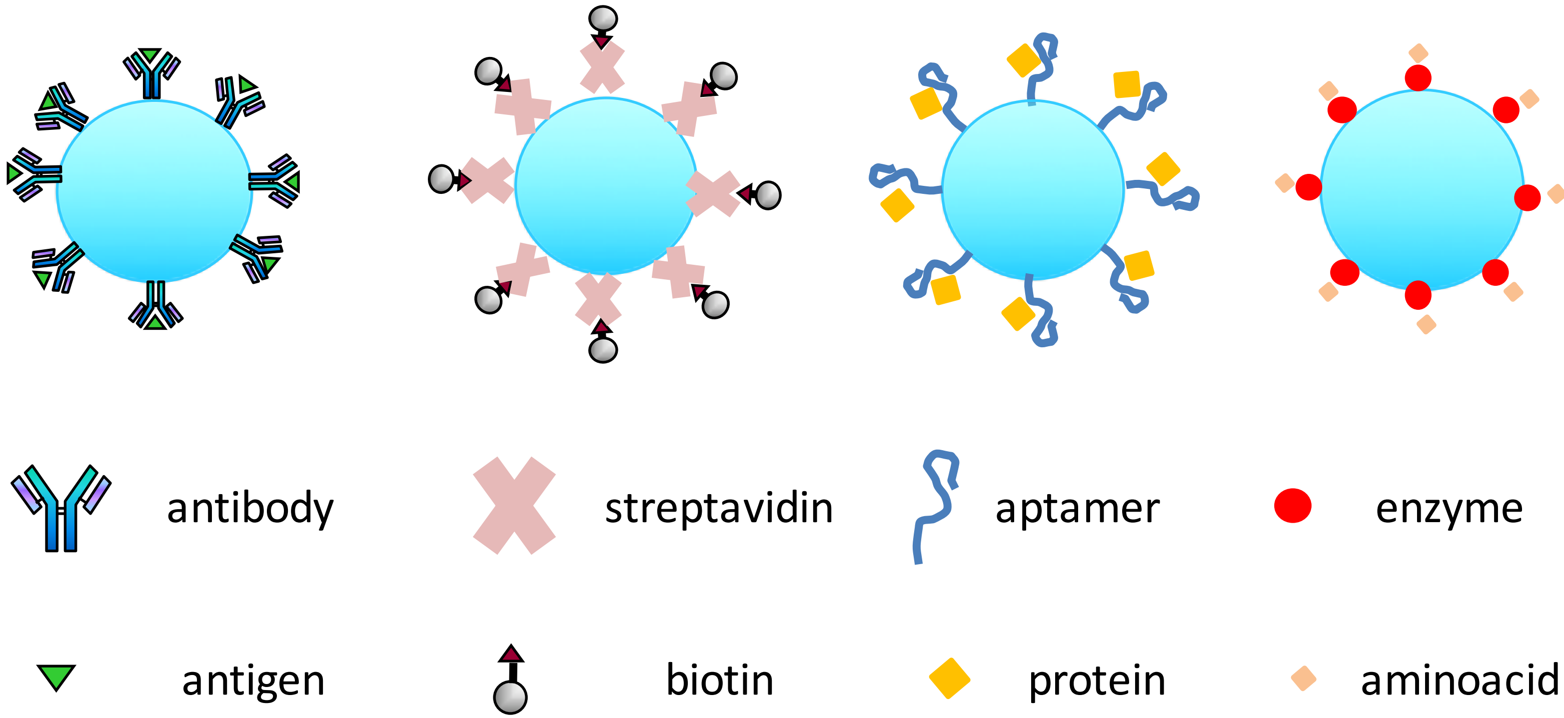

Functionalization of glass microspheres

General Requirements:

- a thickness < 100 nm
- good homogeneity

Possibility to excite WGMs in efficient way by means of evanescent field tail

High Q factor for the (microspheres + coating) structure

IMMUNOSENSING APPLICATIONS

We developed a very easy and repeatable protocol in order to obtain a homogeneous polymeric coating on the surface of the microspheres (2R = 250 μm; ***Q*** > 10^8).

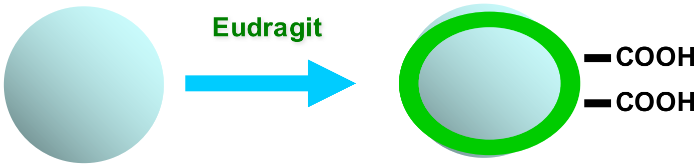

Best concentration for the microspheres functionalization solution: 10 mM l'Eudragit® L100 and 1 mM fluorescein

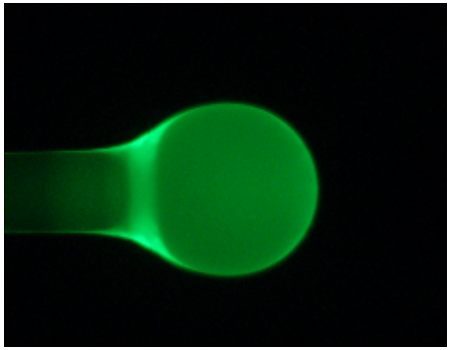

Q = 5.6 x 10^6 in air

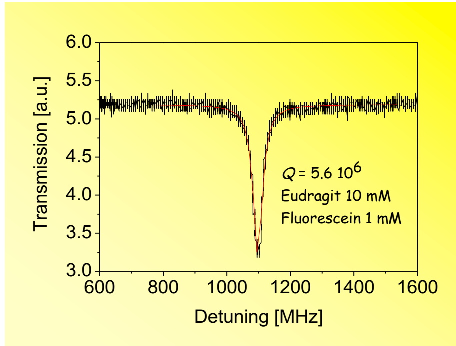

S.Soria et al., Opt. Express, 17 , p. 14694 (2009)

S. Berneschi, et al. "An Introduction to Optoelectronic Sensors", chapter 6, World Scientific Publishing, Singapore (2009)

Functionalization – experimental (ctd)

The next step for the immunosensor realization concerns the antibody immobilization on the functionalized surface of the microresonator. The selected antibody for our investigation was IgG (immuno – gammaglobuline).

Activation of polymeric layers with EDC-NHS chemistry for Eudragit
1-etil-3-(3-dimetilaminopropil) carbodiimide idrocloride (EDC) e *N*-Idroxisuccinimide (NHS)

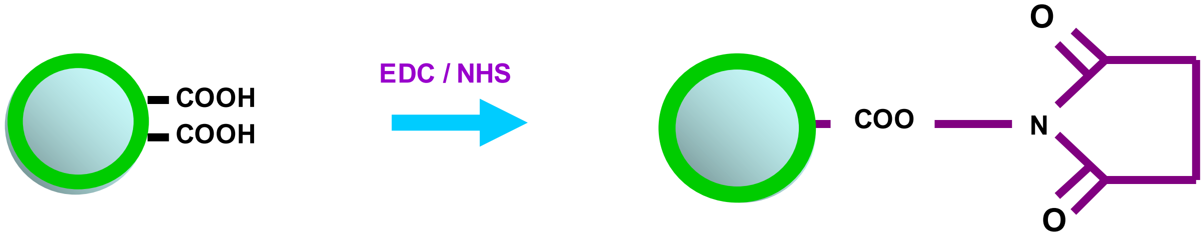

EDC concentration: 2 mM

NHS concentration: 5 mM

activation time: 30 min

Covalent binding of IgG and blocking of active sites with BSA
used concentration of IgG: 0.1 mg / ml

antigen (▼) -- antibody (Y) binding

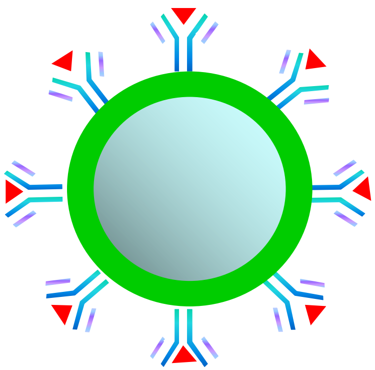

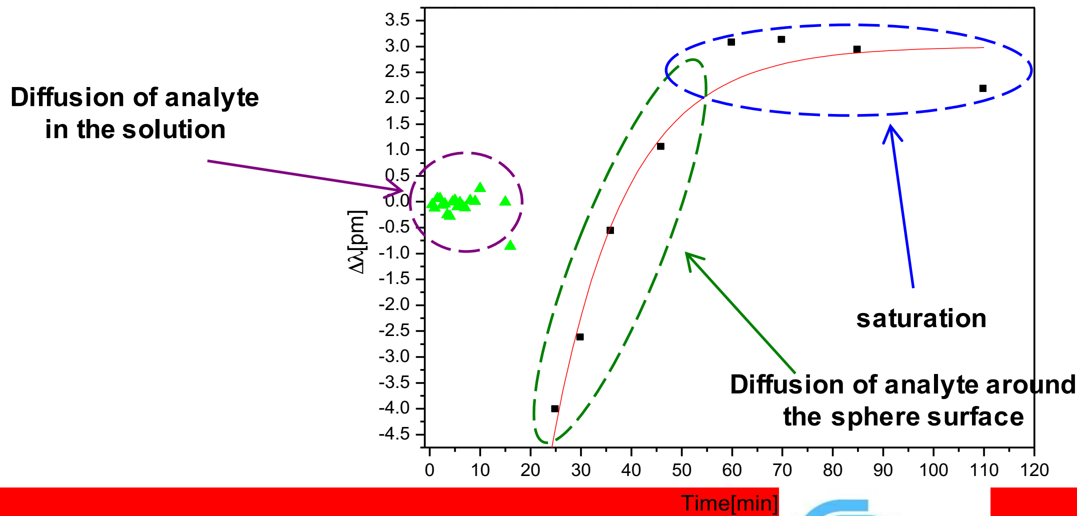

Immunosensor

A resonance wavelength shift ≈ 10.2 ± 0.3 pm after injection of 10 μL of 50 mg·L^{-1} anti-IgG in the PBS solution was measured. Theoretical analysis gave a value for the association constant about 1.9×10^5 $M^{-1}s^{-1}$ for IgG, which is in good accordance with known results for IgG/anti-IgG binding.

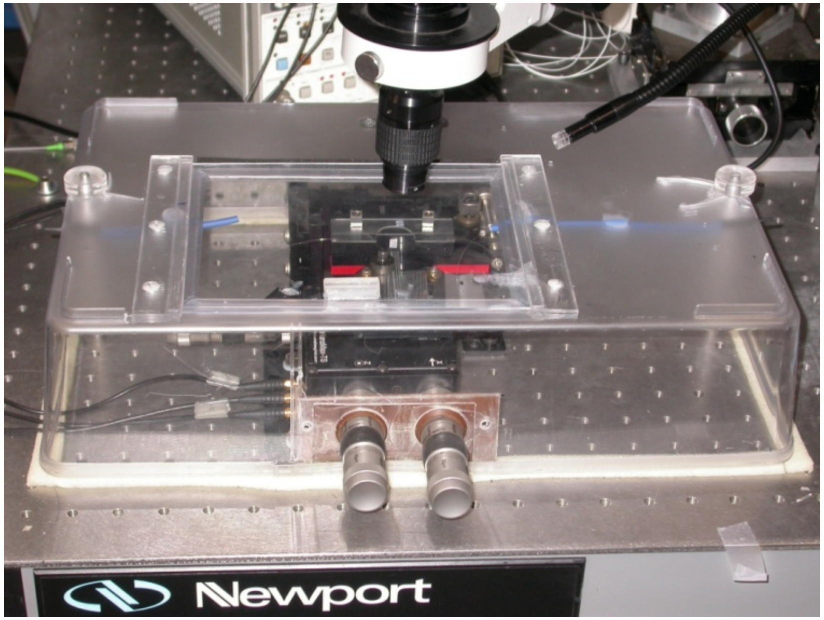

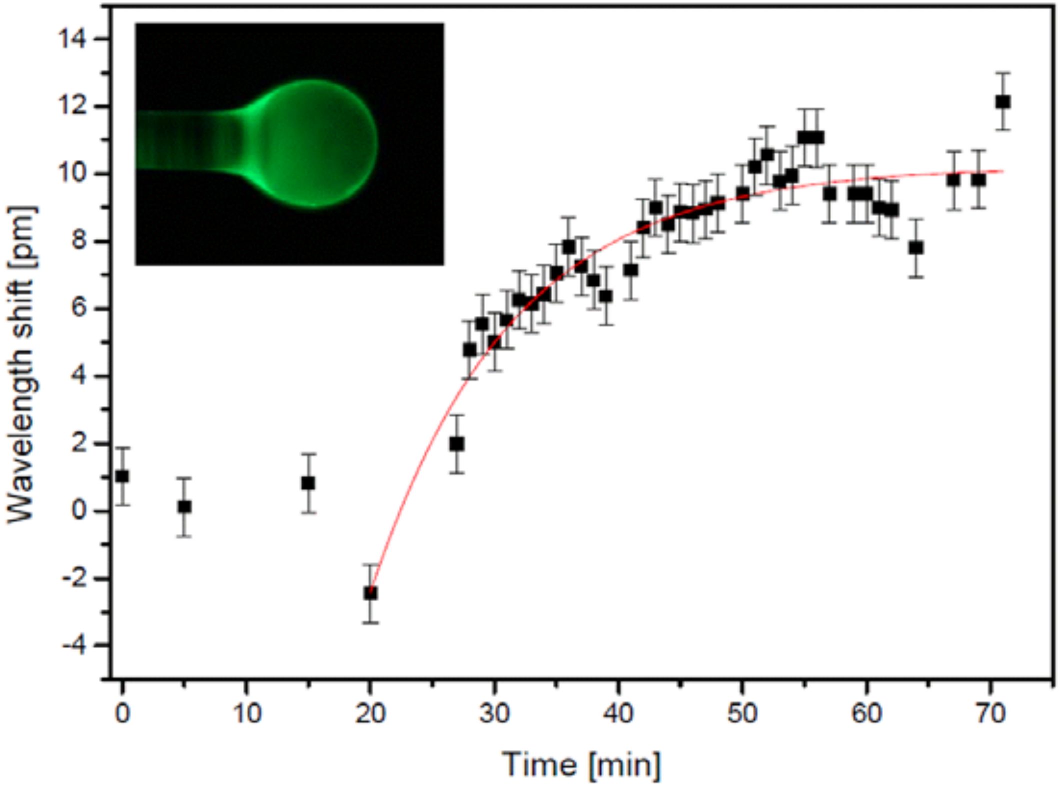

A. Giannetti, S. Berneschi, F. Baldini, F. Cosi, G. Nunzi Conti and S. Soria, "Performance of Eudragit Coated Whispering Gallery Mode Resonator – Based Immunosensors", ***Sensors***, Vol. 12 (2012), 14604-14611.

Aptasensor - functionalization

Another type of immunosensor (therefore called APTASENSOR) uses as bioreceptor APTAMERS, namely RNA or DNA molecules (ca. 30 to 100 nucleotides) that recognize specific ligands and that are selected in vitro from vast populations of random sequences.

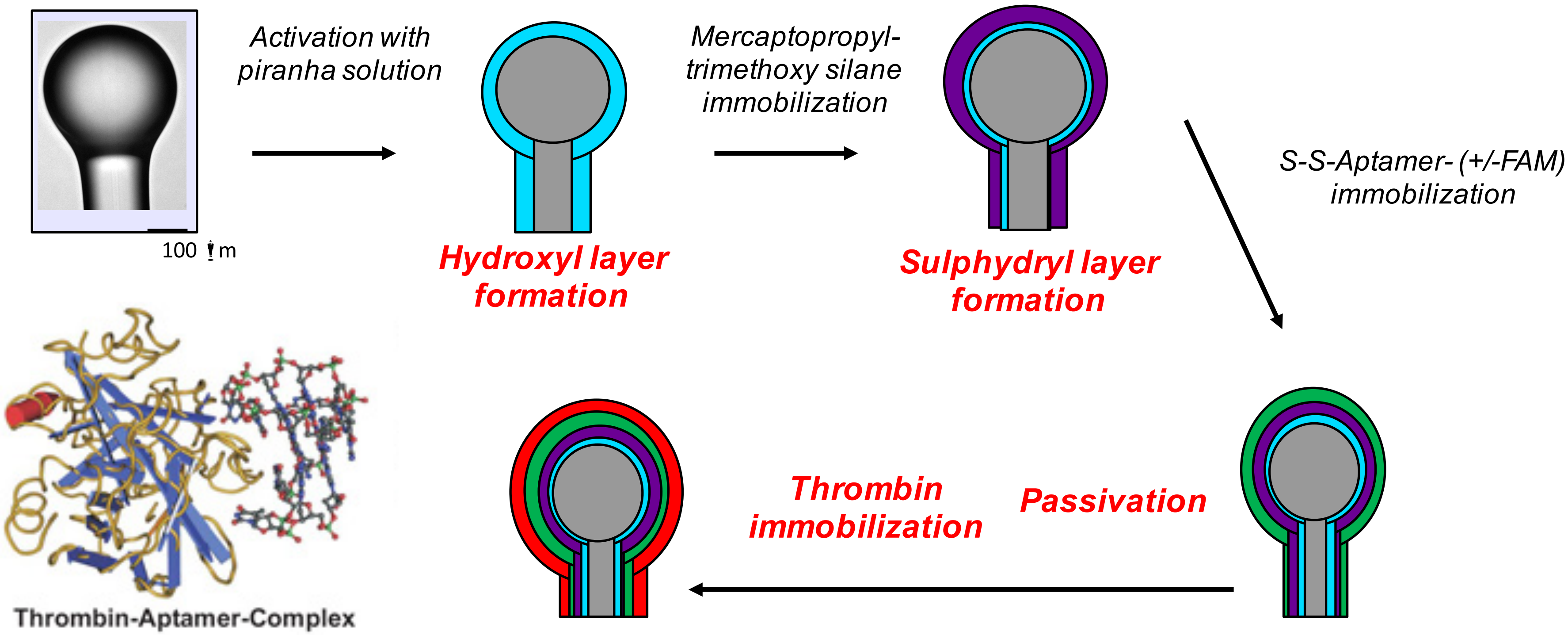

Aptasensing: AFFINITY BINDING APTAMER - THROMBIN

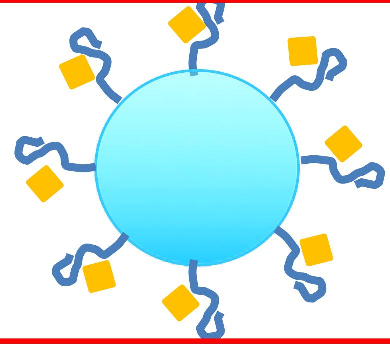

Analysis of the coated microsphere surface, functionalized with MPTMS, aptamer and thrombin, by confocal fluorescent microscopy

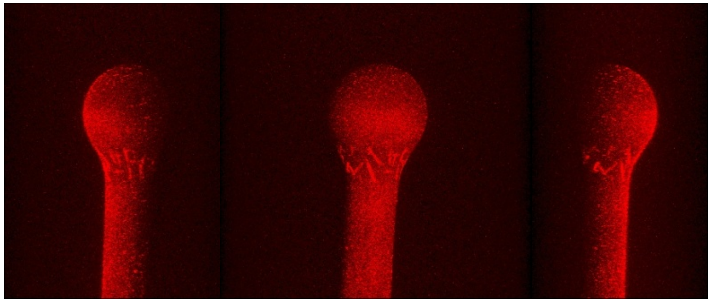

500 µl cell, laminar flow, aptamer chain lenght 15
Thrombin: 40 nM

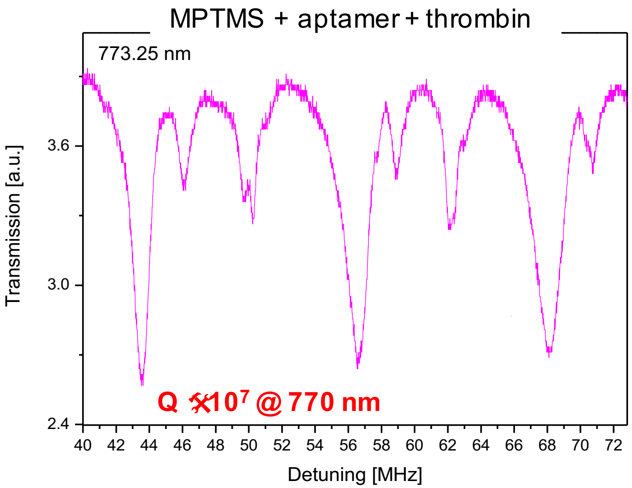

S. Soria et al., ***WGM microresonators for biosensing***, Adv. in Science and Technology, 82 (2013), 55-63.

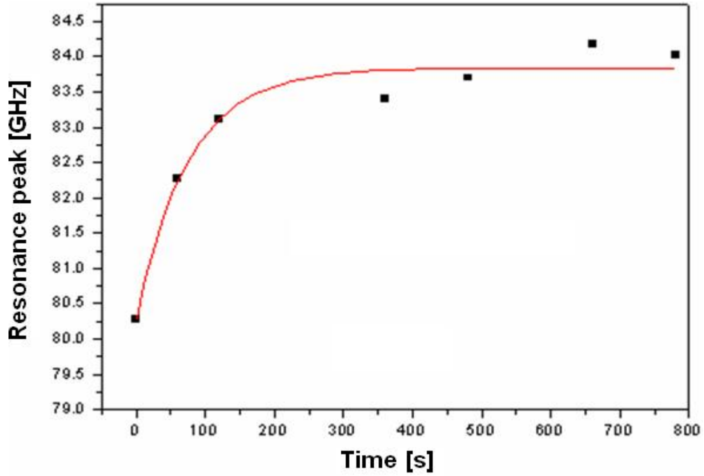

After functionalisation and binding with thrombin: $Q \approx 10^7$ @ 770 nm

The Aptamer – Thrombin binding in PBS solution. The reaction is very fast: after 800 s the saturation condition is reached.

SINGLE VIRUS DETECTION

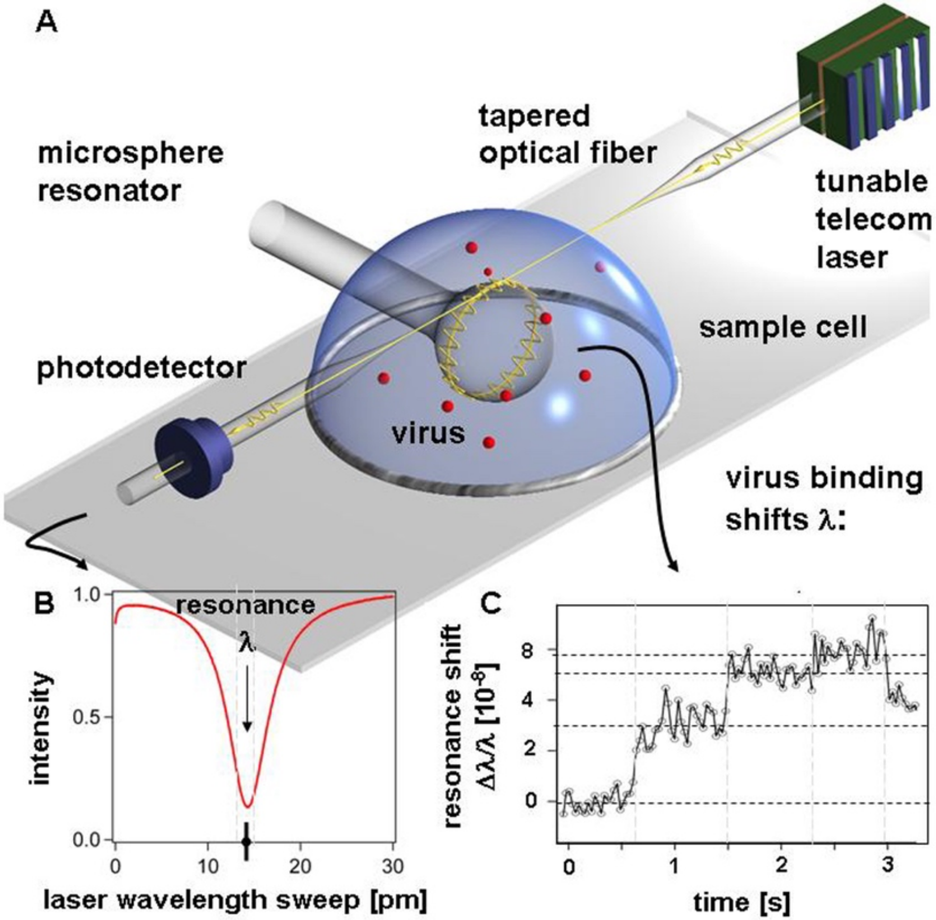

(A) Laser light injected into a fiber and coupled to a glass microsphere.

(B) Resonance signal of glass microsphere with free surface.
Q

C) Ultrasensitive detection of single influenza A virus particles is demonstrated by monitoring changes of the resonance wavelength, and detecting discrete steps in the wavelength-shift signal as virus nanoparticles bind to the microsphere surface.

F. Vollmer and S. Arnold, Whispering gallery mode biosensing: label-free detection down to single molecules, Nat. Methods 5 (7), pp. 591–596, 2007.

F. Vollmer, S. Arnold, and D. Keng, Single virus detection from the reactive shift of a whispering gallery mode, Proc. Natl Acad. Sci. U.S.A. 105 (52), pp. 20701–20704, 2008.

Optofluidics and Microbubble Biosensors

MICROBUBBLE SENSOR

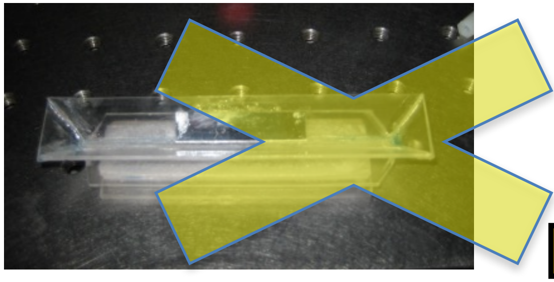

Open fluidic cell

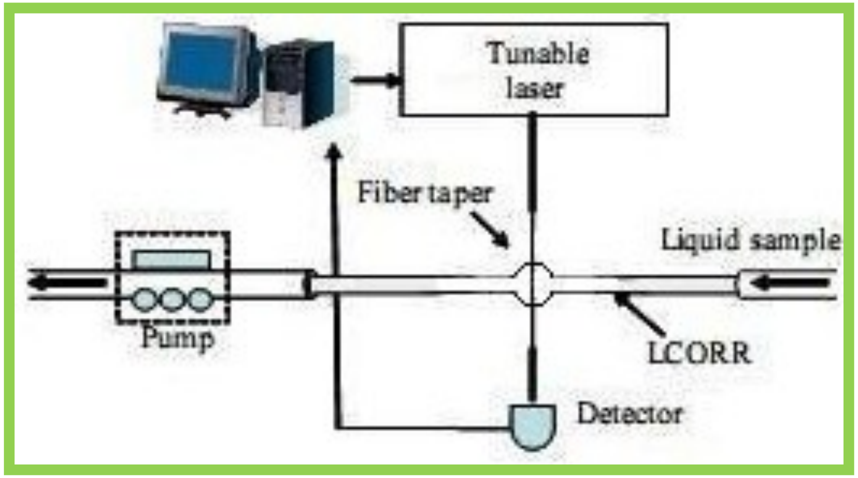

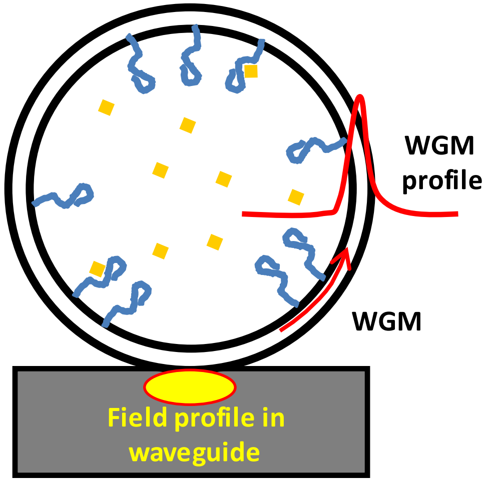

No perturbation in coupling and less breakable structure

M. Sumetsky *et al.*, Opt. Lett. **35**, 898 (2010)

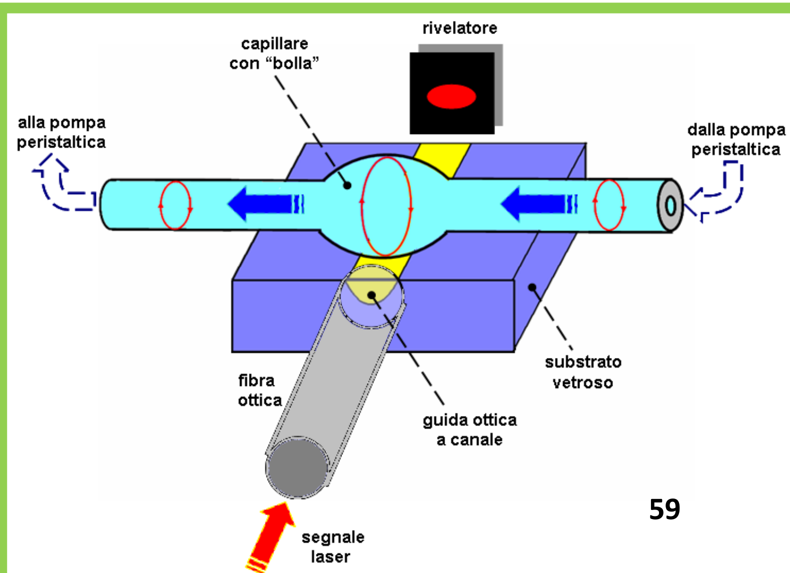

To obtain easily integrable and robust set-up we can combine the microbubble geometry with waveguide coupler.

Microbubble functionalization

A proper chemical solution is flown through the capillary to activate its inner surface by a spatially-selected UV photo-activation (mask).

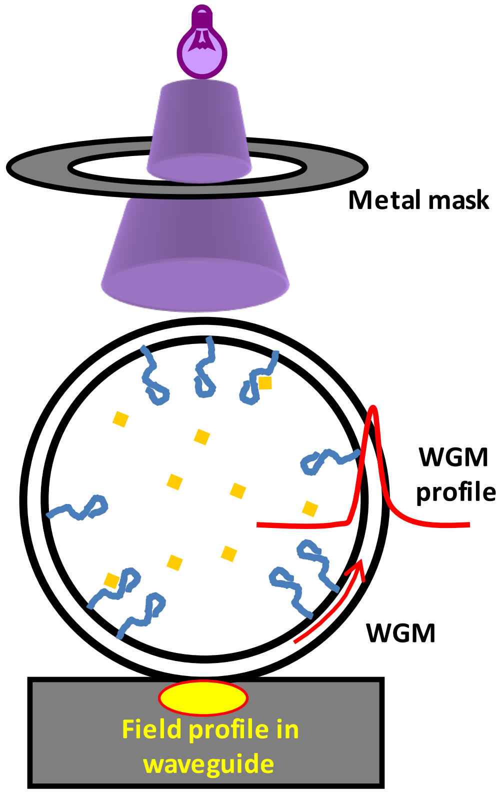

➢ Silanization:

(3-Aminopropyltrimethoxysilane)

* deposition of the activation layer (low selectivity) on the bare WGM resonator;

* covalent binding of the antibody (bioreceptor) to the activation layer (for high selectivity);

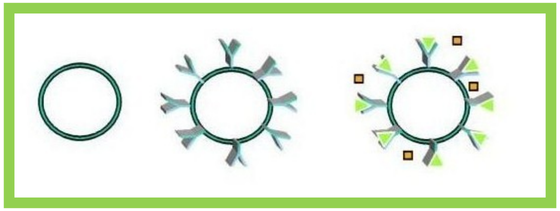

➢ Biotin-streptavidin layer

→ selectivity with one step process

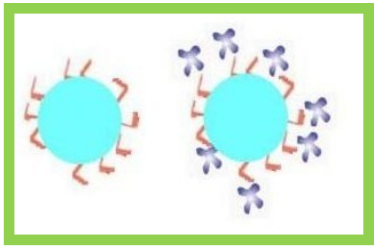

IMPLEMENTATION OF A DEVICE

The development of a real sensing device requires a robust structure, where coupling should not be critical and a fragile tapered fiber would not be convenient.

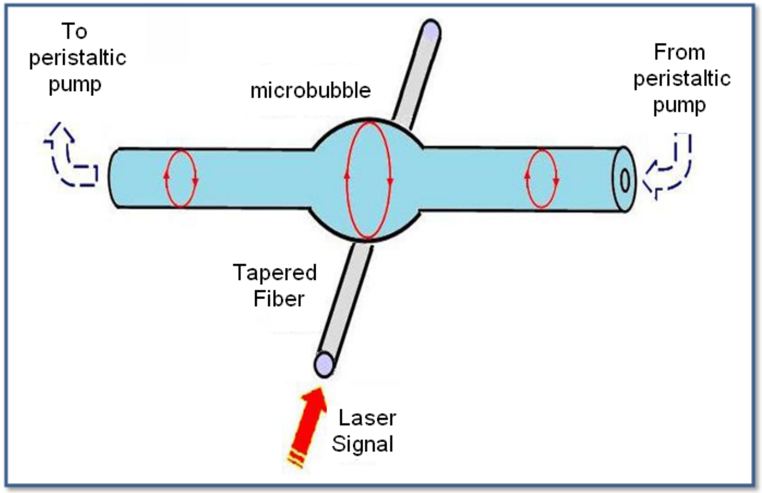

A solution is represented by the coupling with an integrated optical waveguide.

Pro: ***robust***

Con: ***alignment***

(visibility of guide)

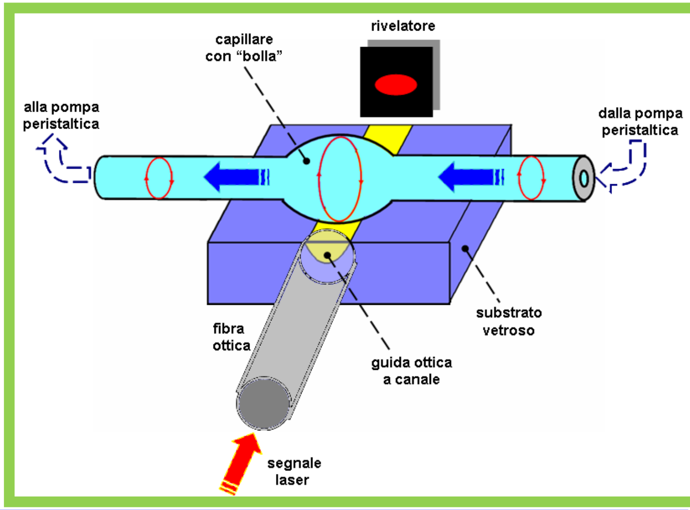

We have considered a different coupling structure, using LPG.

November 15, 2014 / Vol. 39, No. 22 / OPTICS LETTERS

Long period grating-based fiber coupler to whispering gallery mode resonators

D. Farnesi,[1,2] F. Chiavaioli,[2] G. C. Righini,[1,2] S. Soria,[2] C. Trono,[2] P. Jorge,[3] and G. Nunzi Conti[2,*]

[1]*Centro Studi e Ricerche "Enrico Fermi", Piazza del Viminale 2, 00184 Roma, Italy*

[2]*Istituto di Fisica Applicata "N. Carrara", CNR-IFAC, Via Madonna del Piano 10, 50019 Sesto Fiorentino (FI), Italy*

[3]*INESC-Porto, Rua do campo Alegre 687 4169-007, Porto, Portugal*

LPG coupling

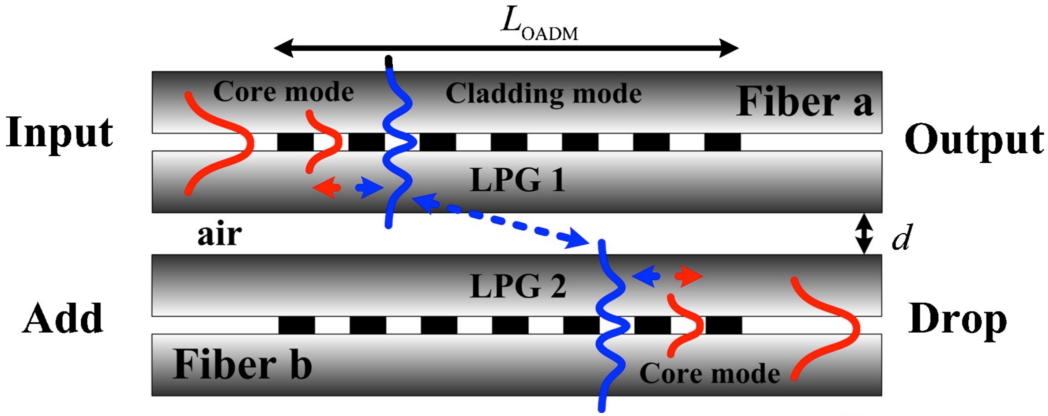

Boron-germanium codoped optical fibers (Fibercore PS1250/1500); point-to-point writing technique; KrF excimer laser (Lambda Physic COMPex 110, λ = 248 nm).

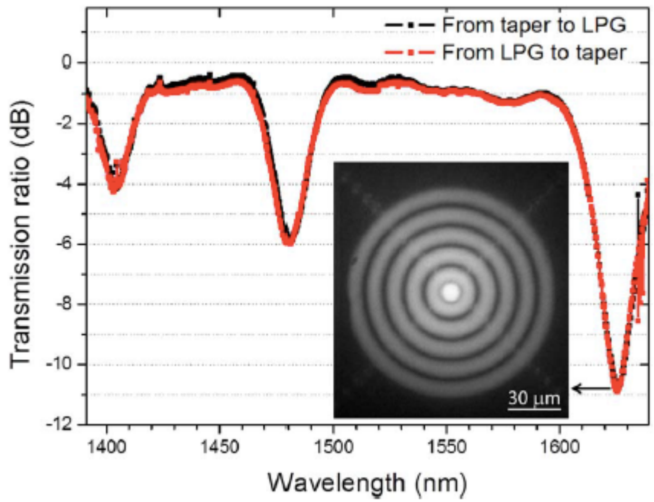

Fig. 1. Transmission spectra of the fiber core through an LPG with a period of 425 µm and a taper of 18 µm. The spectra are measured in both directions. The picture shows the near field intensity image of the LP06 mode associated with the attenuation band around 1625 nm.

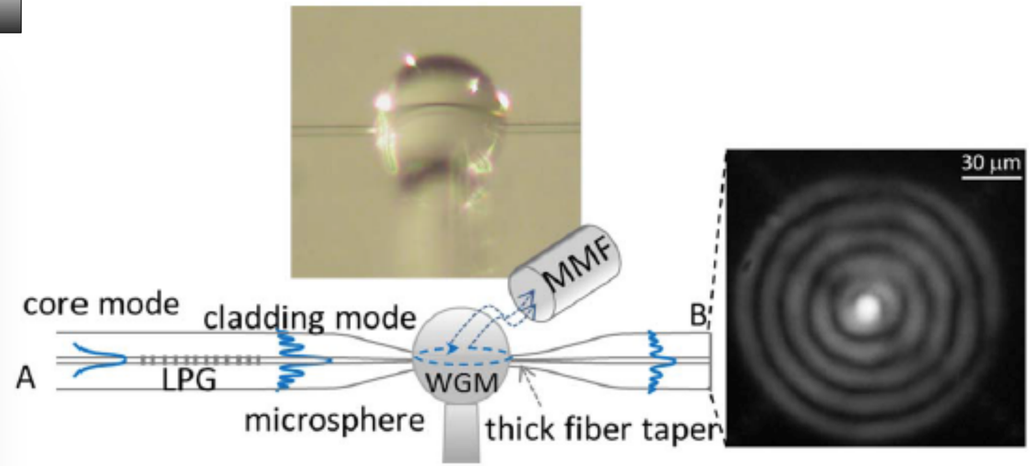

Fig. 2. Sketch of the experimental setup showing the LPG exciting the cladding mode followed by a "thick" taper where coupling with the resonator takes place. The image in the inset shows a 290-µm silica sphere with the fiber taper visible in the background. Light scattered from the microsphere is collected using a multimode fiber (MMF). The picture on the right shows the near field intensity image of the output at 1625 nm.

LPG coupling (2)

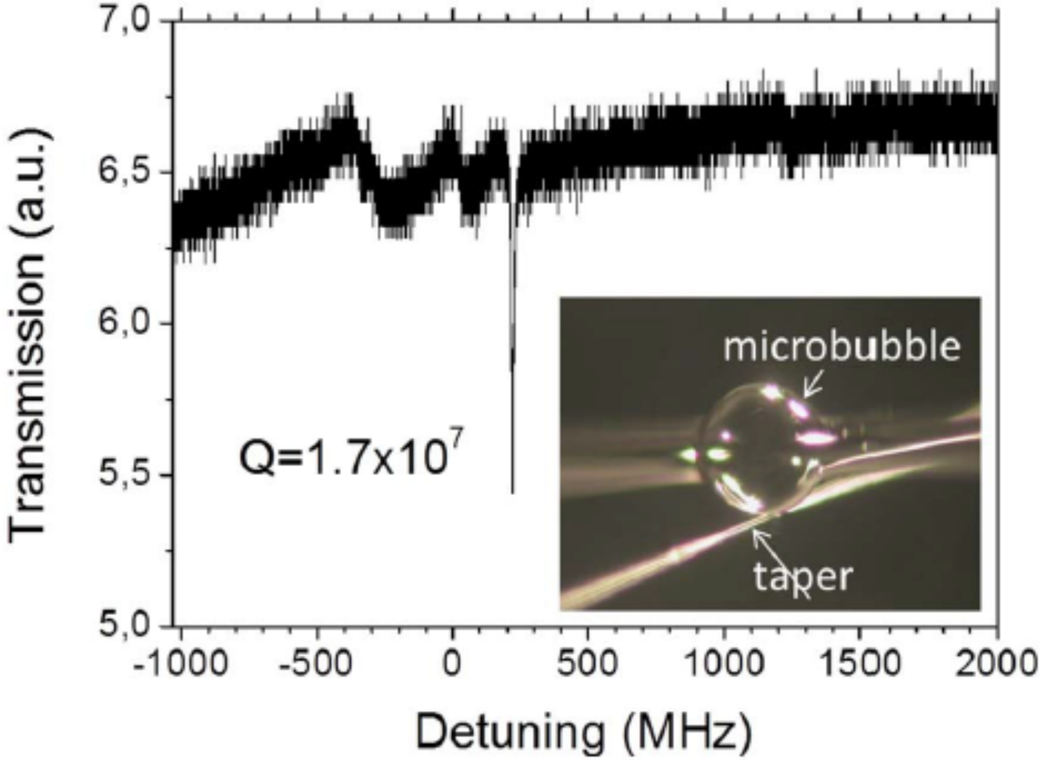

Fig. 4. Example of a WGM resonance excited in a silica microbubble with external diameter of a 490 μm. The inset is an image of the microbubble in contact with the coupling taper.

Then, we considered the possibility of using this approach in order to be able to design a quasi-distributed sensing, using several microspheres.

LPG coupling before & after WGMR

A second LPG, identical to first one, can be inscribed in the fiber after the coupling zone, so to reconvert the cladding modes to the core mode.

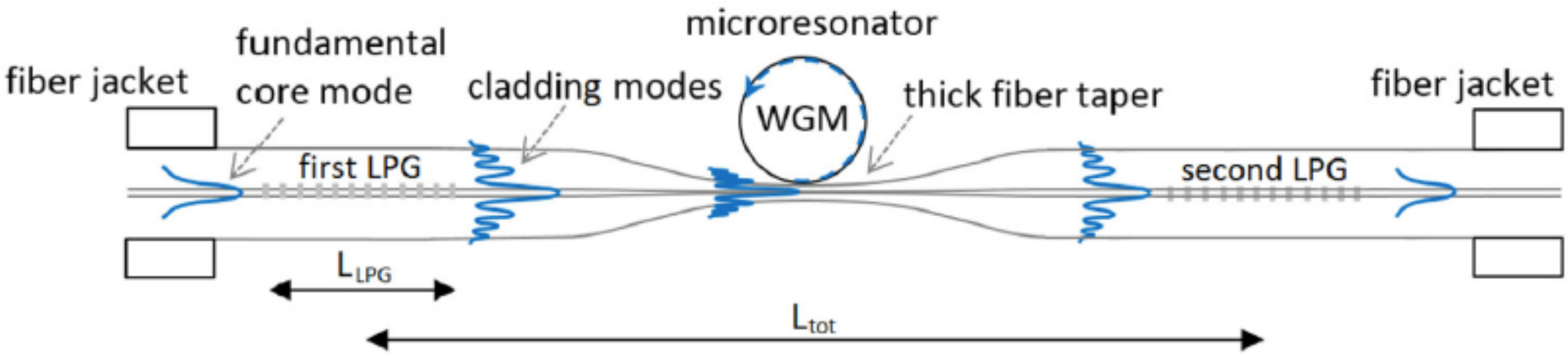

SINGLE FIBER PARALLEL SENSING

The use of this coupling approach allows quasi-distributed and wavelength selective addressing of different micro-resonators along the same fiber.

D. Farnesi et al. , *Quasi-distributed and wavelength selective addressing of optical micro-resonators based on long period fiber gratings*, Opt. Exp. 23, 21175 (10 August 2015)

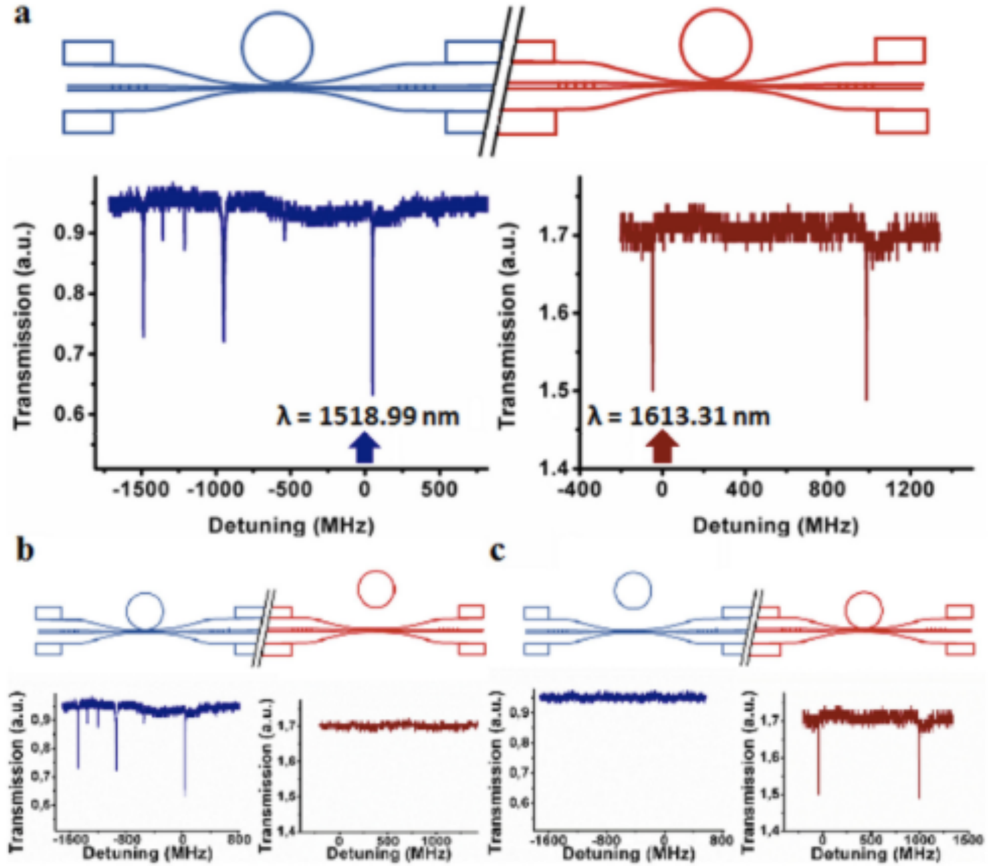

Fig. 4. Sketch of two in series coupling units with both resonators (circle) coupled to each tapered section of the fiber and corresponding resonances obtained by scanning the laser source around the LPGs central wavelengths (0 MHz detuning) (a). First resonator in contact, second not (b). Second resonator in contact, first not (c). The resonances of each coupling unit remain unchanged proving they are independently excited without cross-talk.

CONCLUSIONS

- WGM resonators with very high Q can be routinely produced, and robust coupling system have been tested.
- Very low threshold WGM microlasers, with very narrow linewidth, can be developed.
- Nonlinear optical effects can be quite easily produced in WGM resonators.
- Very-high-sensitivity sensors and biosensors have been demonstrated.

OUTLOOK

A few hot issues:

- Integration and Packaging (e.g. 3D microprinting)
- Advanced configurations (e.g. coupled resonators)
- Combination of WGMR & plasmonics
- Crystalline & hybrid (e.g. silicon core/silica cladding) WGMRs, especially for nonlinear optical devices
- Source of photon pairs and single photons (for quantum computing & quantum cryptography)
- and more exotic devices ….like *living cell* resonators and biolasers for tagging and imaging purposes.

Acknowledgments

Silvia Soria

Gualtiero Nunzi Conti

Daniele Farnesi

Stefano Pelli

Franco Cosi

Simone Berneschi

Francesco Baldini

Ambra Giannetti

Maurizio Ferrari

Alessandro Cosci

and several more : *Andrea Barucci, Alessandro Chiasera, Francesco Chiavaioli, Cecilia Pederzolli, Franco Prudenzano, Davor Ristic, Cosimo Trono….*

CENTRO FERMI
Museo Storico della Fisica e Centro Studi e Ricerche Enrico Fermi


Many thanks for your attention